VR Mediated Teleoperation

Total workspace utilization using null-space projection control

N.S. Hoeba

Technische Universiteit Delft

TUDelft
Delft
University of
Technology

Challenge the future

VR MEDIATED TELEOPERATION

TOTAL WORKSPACE UTILIZATION USING NULL-SPACE PROJECTION CONTROL

by

N.S. Hoeba

in partial fulfillment of the requirements for the degree of:

Master of Science
in Mechanical Engineering

at the Delft University of Technology (TU Delft).

An electronic version of this thesis is available at http://repository.tudelft.nl/.

TUDelft
Delft
University of
Technology

TNO innovation
for life

PREFACE

"Imagination is more important than knowledge. For knowledge is limited to all we know and understand, while imagination embraces the entire world, and all there ever will be to know and understand."
- Albert Einstein

Dear reader,

The quote above is one of the quotes I hold most dear. Not because Albert Einstein said it, but because it describes the way I am. I am a dreamer imagining new ideas, future events, discoveries, etc. Teachers always told me that I should stop dreaming and pay attention to what is happening now. But I disagree. My imagination allows me to understand events, equations, people, ideas that I would never understand with only my knowledge. When I have an idea, I can not tell you exactly what it is. It is more like a feeling, a mix of my imagination, fantasy, knowledge, and dreams which merge creating a stimulus that I perceive as an idea. Only after a substantial amount of time, work, frustration, and guidance, I can exactly tell you what my idea is and why I think it is a good idea.

This also happened when I started my thesis. I had an idea, but I was unable to specify exactly what my idea was. For more than a year, I researched finding the answer to materialize my idea. Working with inspiring people. Being supervised by Ph.D.'s, professors, engineers. People who are all very good at showing me the steps to conduct proper research, materializing ideas, and just having fun. There were also less inspiring moments. The moment when I reached rock bottom was when I was on a beautiful beach in Curacao, but could only think about why I could not exactly define my ideas.

Those moments are behind us, and what we have are 44 pages full of hard work to materialize my idea. I would like to thank Nanda van der Stap and David Abbink for their support, patience, and guidance and of course all other people helping me in converting my idea into this thesis.

Enjoy!

Nirul Hoeba
Delft, August 2019

CONTENTS

1

THE PAPER

VR Mediated Teleoperation: Total workspace utilization using null-space projection control

N.S. Hoeba

Cognitive Robotics, Delft University of Technology, Delft, The Netherlands, n.hoeba@gmail.com

Abstract—**Joint limits and singularities limit the total and intuitive utilization of the robotic workspace in VR mediated teleoperation. This paper presents the development and validation of a novel null-space projection control method, used to adjust joint configurations of teleoperated robot arms containing joint limits and singularities. The novel null-space projection controller enables the operator to manually adjust invalid joint configurations. By doing so, we allow the operator to intuitively utilize the entire workspace of a teleoperated robot arm. A within-subject design experiment assessing operator task performance, acceptance and controller preference of 26 novel operators was executed. The participants were analyzed using the novel and the state-of-the-art end-effector controller for a trajectory following task. The novel controller significantly out-performed the end-effector controller in trajectory accuracy. Operators utilizing the novel controller use significantly less effort when operating the robot arm. The novel controller was also rated significantly more useful and satisfying than the end-effector controller, resulting in 81% of the participants preferring the novel controller over the end-effector controller. Further development and future studies will explore the full capabilities of the novel controller, improve performance, user acceptance and explore additional applications.**

I. INTRODUCTION

In telerobotics, optimal operator skill utilization requires full manipulation capabilities to intuitively utilize the total workspace of the robot arm. In previous studies [1] [2], it was shown that full operator manipulation capabilities are not yet attained due to the non-intuitive control by the result of invalid joint configurations. Invalid joint configurations are joint configurations which contain internal singularities (henceforth referred at as singularities) or joint limits [3]. When operating a robot arm, invalid joint configurations are attained because the (operational) workspace of a robot is not transparent or intuitively understood by the operator controlling the robot. Therefore operators are unaware of the boundaries and limits of the robot workspace. Invalid joint configurations in combination with the opacity of the workspace boundaries prevent intuitive operation or the ability to control the robot arm without the need for extensive training with robotic arms [4]. In this research, we try to enable intuitive and total workspace utilization using VR mediated teleoperation.

The VR mediated teleoperation framework combines telepresence and teleoperation by the use of a virtual reality (VR) environment [2]. Utilization of the VR environment enables us to create a virtual shared world between the operator and the slave robot. In this framework, both the operator and the slave robot operating at a remote environment are virtually present. In state-of-the-art teleoperation frameworks, operators have to use multiple two-dimensional displays to interpret the environment, states, and workspace of the robot. It is believed that the implementation of VR in teleoperation increases telepresence, improving the interpretability of the remote environment. Increased telepresence presents higher dimensionality in spatial information of the remote environment compared to two-dimensional displays [2] [5]. Using VR in teleoperation provides the human operator with full perceptual capabilities to intuitively perceive the remote environment, to act as if being present at the remote site. Combining the cognitive ability of the human operator with the robotic capabilities at a distance [6].

State-of-the-art VR mediated teleoperation utilizes end-effector control to move the robot through its workspace. End-effector control indicates the translation and rotation of only the end-effector using a master device. As validated in [2], end-effector control induces accurate and intuitive operation in the sections of the workspace where the probability of attaining an invalid joint configuration is low. In the regions where this probability is higher, because the operator can only manipulate the robotic end-effector and not its joint configuration, translocation through the workspace results in the termination of the end-effector movement when invalid joint configurations are attained [4]. For the KUKA LBR iiwa 7, invalid joint configurations result in the termination of movement when moving from the front to the back of the workspace. This results in some sections of the workspace to be difficult and not intuitive to reach. To allow the operator to intuitively utilize the total workspace we should, next to moving the end-effector through its workspace using end-effector control, allow the operator to directly adjust the joint configuration of the robot to adjust invalid configurations to valid configurations.

A. Related work

In literature, methods which adjust invalid joint configurations to valid joint configurations use a projection on the null-space [4] [7]. The null-space is a mathematically well-defined space. It describes the motion a robot arm can make without moving the end effector. A projection on the null-space with

a vector in the joint-space results in the removal of the vector parts that results in end-effector motions.

In the research of [8], a redundancy-resolution algorithm is introduced that uses an orthogonal projection based on the instantaneous geometry of the task. In the research of [8] and [7], the projection on the null-space is used to correct invalid joint configurations. In the study of [8], the algorithm has the task to autonomously follow a predefined trajectory to weld a certain area. When the robot follows this trajectory, it encounters invalid joint configurations causing it to deviate from the predefined trajectory. Because of this unwanted behavior of the algorithm, an orthogonal projection or a null-space projection method is used to resolve these invalid joint configurations. This enables the robot to follow the predefined trajectory without having to deviate from this trajectory.

Alongside the usage of null-space projection controllers in autonomous tasks, null-space projection controllers are also used in semi-autonomous tasks, e.g. shared and cooperative control. Shared control is the control of an automated system where a human controller shares physical (e.g. haptic) control with an automatic controller to achieve a common goal. Both the operator and the algorithm have knowledge about each other's possibilities and limitations on an operational level. Cooperative control, a concept nested with shared control focuses on the achievement of a common goal on higher levels, which are tactical and strategic levels [9] [10]. According to [10], cooperation can include shared control, but there can be cooperation without shared control.

In the study of [11] and [12], the operator is accountable for a set of tasks (e.g. following a trajectory or translating the end-effector from point A to B). The null-space projector controller is accountable for correcting invalid joint configurations. Resulting in the algorithm and the operator to share control. In the study of [4], cooperative control is used to avoid singular configurations. When the arm is close to a singular posture, the arm trajectory is stopped and the operator is given the possibility to choose from the valid joint configurations to avoid a singularity by manually adjusting the configuration.

B. Objective and Contribution

In the current VR mediated teleoperation system, end-effector movement through the workspace of the robot, results in the termination of the end-effector movement when invalid joint configurations are attained. Causing some parts of the workspace to be not intuitive and difficult to reach. Next to the usage of null-space projection controllers in autonomous and semi-autonomous tasks, integration of null-space projection controllers in the VR mediated teleoperation of the robot arm could be beneficial. Because VR mediated teleoperation requires manual adjustment of invalid joint configurations, by our knowledge no algorithm available in the literature is

suitable for VR mediated teleoperation.

The objective of our study is to develop and validate a control algorithm suitable for VR mediated teleoperation of a redundant KUKA LBR iiwa 7 robot arm used in free-air movement applications to enable intuitive and total workspace utilization. Free-air movement applications are applications where the robot is moving through its workspace without interacting with other objects. These applications are chosen because of the frequent occurrence of these applications in the teleoperation of robot arms. These can be applications in sea, space and on land. Varying from domains in the chemical industry to healthcare and defense. Use cases can be found in translocating radioactive material in hazardous environments like a nuclear plant, where total and intuitive workspace utilization is critical for safe and fast completion of the task [2] [13]

This study contributes to 1) enabling the operator to intuitively utilize the total workspace. 2) The analysis of operator performance, acceptance, and preference when operating a robot arm. 3) The further development of the VR mediated framework for intuitive teleoperation.

This paper is organized as follows. The second section gives a brief overview of the modeling methodology of the controllers and the human subject experiment methodology. The third section presents the results of the human subjects experiments. The main results and the limitations of our approach will be discussed in the fourth section. Our conclusions are drawn in the final section.

II. METHODOLOGY

A. Definitions

This section clarifies the definitions used in the modeling methodology (Section II-B), to explain the working principle of the developed controllers.

Let $\mathfrak{J}$ denote the *joint space* of a robot arm containing $n + 1$ rigid bodies serially connected by n revolute (R) joints. The joint configuration of the robot arm in $\mathfrak{J}$ is given by a vector $\boldsymbol{\theta}$, so that $n = dim(\mathfrak{J}) = dim(\boldsymbol{\theta})$. The KUKA LBR iiwa 7 arm consists of $n = 7$ revolute joints, and $n + 1 = 8$ rigid bodies (Fig. 1). Joint configuration vector $\boldsymbol{\theta}$ is given by:

$$\boldsymbol{\theta} = \begin{bmatrix} \theta_{R1} & \theta_{R2} & \theta_{R3} & \theta_{R4} & \theta_{R5} & \theta_{R7} \end{bmatrix}^T \qquad (1)$$

Where θ_{R1} until θ_{R7} denote the joint angles for all 7 DOF's. Because an unconstrained rigid body in space can have at most six DOF's (i.e. three translations and three rotations), the *operational space* of the end-effector is denoted by $o = dim(\mathfrak{O}) \leq 6$ and the *task space* of the end-effector is defined by $t = dim(\mathfrak{T}) \leq 6$. Using the operational and task space of the end-effector, we can define three definitions which are *intrinsic*, *functional* and *kinematic redundancy*. According to [8], a serial manipulator is *intrinsically redundant* if the $n =$

$dim(\mathfrak{J})$ is greater than $t = dim(\mathfrak{T})$. The degree of *intrinsic redundancy* is given by (2).

$$r_I = n - o \tag{2}$$

For the KUKA LBR iiwa 7 robot arm, $r_I = 7 - 6 = 1$. *Functional redundancy* denotes a pair of serial manipulator tasks where the $o = dim(\mathfrak{O})$ is greater than $t = dim(\mathfrak{T})$ as given in (3), where $\mathfrak{T}$ is a subset of $\mathfrak{O}$. i.e $\mathfrak{T} \subseteq \mathfrak{O}$.

$$r_F = o - t \tag{3}$$

Kinematic redundancy denotes a pair of serial manipulator-task where $n = dim(\mathfrak{J})$ is greater than $t = dim(\mathfrak{T})$ as given in (4), where again $\mathfrak{T}$ is a subset of $\mathfrak{O}$. i.e $\mathfrak{T} \subseteq \mathfrak{O}$.

$$r_K = n - t \tag{4}$$

Substitution of (2), (3) in (4) result in (5), which denotes that kinematic redundancy derives from two sources namely *intrinsic redundancy* and *functional redundancy*.

$$r_K = r_I + r_F \tag{5}$$

A broader definition or more information about the redundancy of serial manipulators can be found in [8].
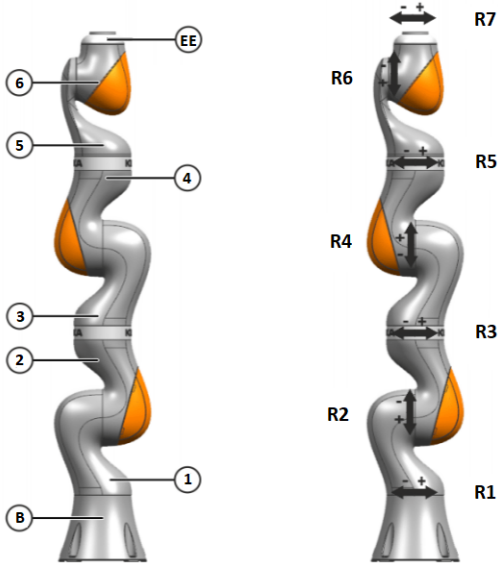

Fig. 1: (left) visual representation of the 8 rigid bodies of the KUKA LBR iiwa 7. (right) Visual representation of the 7 DOF's revolute joints of the KUKA LBR iiwa 7.

B. Modelling

1) Teleoperation: A telerobotic system controlling a robot arm consists of two main parts. A human controlled master device, which detects the motions of the operator, and a slave robot controlled by the master device executing these motions. The VR mediated teleoperation framework (Fig. 5) is divided into a slave system and a master system. The master system consists of an master device called the HTC Vive virtual reality system and a VR environment. The HTC Vive VR system is implemented as master device in the VR mediated framework because of its low purchase cost with respect to other slave devices, excellent implementation capabilities in VR, its portability options, low setup time and the possibility to provide visual and tactile feedback [5]. The HTC Vive VR system consists of two control devices and one head-mounted display (HMD). The control devices have multiple input methods which include a multi-functional trackpad, grip buttons, and dual-stage triggers. The pose of the control devices is determined using 24 infrared sensors with update rates ranging from 250Hz to 1kHZ [14]. The HMD is used by the operator to visualize the VR environment. A Windows computer is utilized to build and host a virtual reality (VR) environment in Unity. A change in pose of the control devices results in a motion command which is sent to the VR environment.

The VR environment contains a virtual humanoid avatar and a virtual robot arm. This VR environment enables the possibility for the operator to interact with the slave robot as being present at the same location. Telepresence is realized by the transfer of human motion to the virtual humanoid avatar. This transfer is accomplished by the use of the HTC Vive controllers and the HMD to track human hand and head motions. Due to this transfer, the operator does not only see the VR environment but also controls the virtual body as its own. All motion information is transferred to the inverse kinematic solver [15] which derives an estimate for the motion of all virtual body parts. The motion command generated by the control devices is sent via the VR environment to the slave system.

The slave system consists of a slave robot arm and a Linux computer to build and host the robot control algorithms henceforth referred to as *controllers*. The KUKA LBR iiwa 7 slave robot arm is a lightweight 7-DOF robot arm having a reach of 800-820 mm (Fig. 1). In this study, instead of a real robot, the slave system communicates with a virtual robot which acts as a real robot. This virtual duo is used instead of a real robot to firstly, provide easy and safe testing and secondly, provide portability of the total system. The (virtual) robot is programmed using ROS Kinetic [16] and visualized in a robot simulation environment called Gazebo [17]. Using the motion command of the master system, the controllers in the slave system convert the motion command to a robot arm joint trajectory. After conversion, the joint trajectory is sent to the master system. In the VR environment, the joint trajectory is executed by the virtual robot which is observed by the virtual avatar. This observation is provided as visual feedback to the operator using the HMD. Hereafter the operator can use the control devices for a new motion command.

2) Control Scheme: The (virtual) robot can be controlled using two different control modes. These control modes are *end-effector control* and *null-space control*. Conversion from

one control mode to another is carried out using the HTC Vive control devices and is enabled using the dual-stage triggers on the master devices. This section will briefly explain the working principles of both control modes.

a) End-effector control: The motion of the control device operated by the right hand is linearly mapped to the end-effector of the virtual robot. For the sake of numeral computation, we replace velocities for small displacements [8] [18].

$$\dot{\boldsymbol{\theta}} \rightarrow \Delta \boldsymbol{\theta}$$
$$\dot{\boldsymbol{x}} \rightarrow \Delta \boldsymbol{x} \tag{6}$$

The Jacobian matrix of a 7-DOF redundant manipulator is denoted by $\mathbf{J}$. $\mathbf{J}$ is a matrix which describes how joint motions result in end-effector motions. The amount of rows of a $\mathbf{J}$ is equal to the six DOF's of the end-effector. The amount of columns of a $\mathbf{J}$ is equal to $n = dim(\mathfrak{J})$. We need all six rows of $\mathbf{J}$ to fully define the pose of the end-effector in space resulting in $t = dim(\mathfrak{T}) = 6$. Using the resolved motion-rate method proposed by [18], the joint configuration displacement vector concerning this linear mapping is given in (7).

$$\Delta \boldsymbol{\theta} = \mathbf{J}^{\dagger} \Delta \boldsymbol{x}$$
$$\Delta \boldsymbol{x} = (\boldsymbol{x}_{sp} - \boldsymbol{x}_{ee}) \tag{7}$$

Here, $\mathbf{J}^{\dagger}$ is the pseudo-inverse matrix of $\mathbf{J}$. $\boldsymbol{x}_{sp}$ is the 7×1 joint pose vector of a set-point and $\boldsymbol{x}_{ee}$ is the 7×1 joint pose vector of the end-effector configuration. The first three rows of $\boldsymbol{x}$ denote the three-dimensional position of the end-effector. The last four rows represent the orientation of the end-effector in quaternion form. The new joint configuration vector $\boldsymbol{\theta}_{post}$ denotes the joint configuration after addition of the $\Delta \boldsymbol{\theta}$ to the previous joint configuration $\boldsymbol{\theta}_{pre}$ of the robot.

$$\boldsymbol{\theta}_{post} = \boldsymbol{\theta}_{pre} + \Delta \boldsymbol{\theta} \tag{8}$$

$\boldsymbol{\theta}_{post}$ is used as input for the robot to translate the end-effector equal to the translation of the control device. After the robot executes the new joint trajectory, $\boldsymbol{x}_{ee}$ is given as output which is used in the next iteration.

b) Null-space projection control: The null-space projection controller utilizes the null-space of $\mathbf{J}$ to adjust joint configurations containing internal singularities and joint limits. To adjust joint configurations containing joint limits, in the optimal case $r_K = 7$. In this case, we can manipulate every joint configuration separately. Because the end-effector is not constrained in space, we can adjust the joint configuration by adding $\Delta \boldsymbol{\theta}$.

$$\boldsymbol{\theta}_{post} = \boldsymbol{\theta}_{pre} + \Delta \boldsymbol{\theta}_{sp} \tag{9}$$

Here, $\Delta \boldsymbol{\theta}_{sp}$ represents the joint displacement vector for a joint configuration set-point defined by the operator. To adjust the current joint configuration $\boldsymbol{\theta}_{pre}$, resulting in the new joint configuration $\boldsymbol{\theta}_{post}$. Although a dimension of the task-space equal to zero is optimal for the adjustments of joint configurations containing joint limits, task spaces greater than zero are more frequently encountered [7] [8].

In our study, teleoperation is related to the translation of the end-effector resulting in a task-space with a dimension of three ($t = dim(\mathfrak{T}) = 3$), a functional redundancy of three ($r_F = 3$), resulting in a kinematic redundancy of four ($r_K = 4$). Because $t = 3$, we are only interested in the $\mathbf{J}$ that describes how a joint configuration vector results in the x,y,z motion of the end-effector. The Jacobian which describes this motion is defined as $\boldsymbol{J}_p$. Solving (10) results in $\boldsymbol{N}_{J_p}$, denoting the 7×4 null-space matrix of $\boldsymbol{J}_p$. Using $\boldsymbol{N}_{J_p}$ we can derive a joint angular velocity vector which adjust the robot arm joint configuration for a fixed end-effector position. The joint angular velocity vector $\dot{\boldsymbol{\theta}}_{ns}$ member of the $\boldsymbol{N}_{J_p}$ subspace is given in (11).

$$0 = \boldsymbol{J}_p \dot{\boldsymbol{\theta}} \tag{10}$$

$$\dot{\boldsymbol{\theta}}_{ns} = \boldsymbol{N}_{J_p} \xi \tag{11}$$

ξ is an 4×1 arbitrary vector, and requires integer values between -1 and 1 (12) . These values denoted by k (13) adjust the configuration of four joint groups in the null-space of the robot arm in respectively clockwise and counterclockwise direction. Together (12) and (13) show all possible values ξ can attain to adjust invalid joint configurations.

$$\xi \begin{cases} \begin{bmatrix} k & 0 & 0 & 0 \end{bmatrix}^T \\ \Rightarrow R1, \ R2, \ R3 \\[6pt] \begin{bmatrix} 0 & k & 0 & 0 \end{bmatrix}^T \\ \Rightarrow R2, \ R4, \ R6 \\[6pt] \begin{bmatrix} 0 & 0 & k & 0 \end{bmatrix}^T \\ \Rightarrow R1, \ R4, \ R5 \\[6pt] \begin{bmatrix} 0 & 0 & 0 & k \end{bmatrix}^T \\ \Rightarrow R7 \end{cases} \tag{12}$$

$$k \begin{cases} 0 \\ 1 \\ \text{-}1 \end{cases} \tag{13}$$

Addition of $\dot{\boldsymbol{\theta}}_{ns}$ with the current joint configuration $\boldsymbol{\theta}_{pre}$ results in the adjustment of the joint configuration for a fixed end-effector position as in (14). dt is the time between two consecutive iterations.

$$\boldsymbol{\theta}_{post} = \boldsymbol{\theta}_{pre} + \dot{\boldsymbol{\theta}}_{ns} dt \tag{14}$$

(11) with $\xi = \begin{bmatrix} k & 0 & 0 & 0 \end{bmatrix}^T$ and $k = 1$ will result in the counterclockwise rotation of the robotic joint configuration with a fixed end-effector position as denoted in (12) and visualized in Fig. 2.
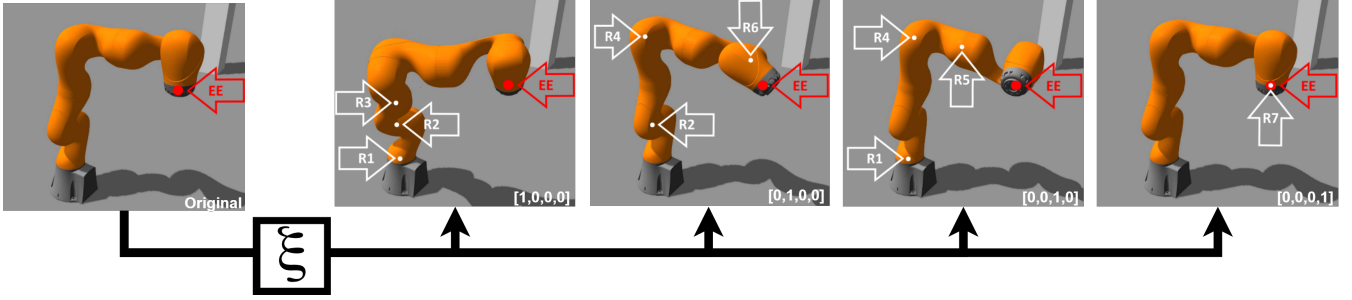
5

Fig. 2: Adjustment of the robot joint configuration using a projection on the null-space with a vector ξ. Resulting the possibility to adjust four joint groups. Group 1 contains joint 1, 2 and 3. Group 2 contains joint 2, 4 and 6. Group 3 contains joint 1, 4 and 5. Group 4 contains joint 7. In this figure, the red arrow indicates a rigid body fixed in space. The white arrow indicates a joint accountable for the change in robot joint configuration with respect to its original joint configuration.
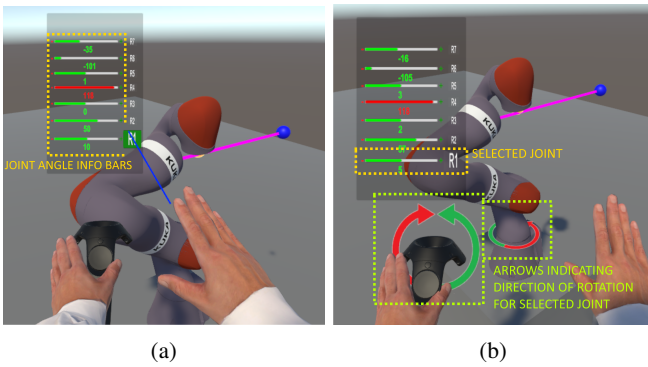

(a)　　　　　　　　　(b)

Fig. 3: An interface used in the VR mediated teleoperation tasks to select joints and observe joint states when utilizing the novel controller.

3) Interface: According to [8], the first step in avoiding singularities is to detect them in the joint space. The same statement can be made in avoiding joint limits. An interface (Fig. 3) is created to provide unilateral visual and tactile feedback to notify the operator when invalid joint configurations are attained. Tactile feedback is utilized to notify the operator, where visual feedback provides information about which kind of invalid joint configuration is attained. This interface utilizes unilateral feedback because this study focuses on the translation of the end-effector through the workspace (free-air movements) disabling the possibility for bilateral feedback. Unilateral feedback is necessary because unlike the (semi-)autonomous controllers in [8] and [7] the operator does not intuitively understand the limits of the robotic workspace. Where (semi-)autonomous controllers are notified that a threshold is breached and the configuration becomes invalid, the operator is not. The interface provides a functional tool for the operator to act appropriately to the source of the invalid configuration.

Due to the usage of the novel controller, the operator can utilize the total robotic workspace. The operator can control the joint configuration of the robot directly to work around invalid configurations. This was indirectly or not intuitively possible when using the end-effector controller resulting in the robot arm to stall in certain areas of its workspace.

C. Human Factor Study

The novel controller is validated with a within-subjects experiment. The experiment has the objective to quantify the difference in operating performance between the operator utilizing the state-of-the-art end-effector controller and the novel controller in a free-air movement application. To allow intuitive and total workspace utilization.

The free-air movement application associated with this experiment is a trajectory following task. In this task, the operator should operate the robot's end-effector to track a predefined trajectory as accurately as possible. We focus on trajectory accuracy because according to [2], accuracy in the manipulation of the robot in a remote environment is essential when the operator holds an executive position over the robot arm manipulator. In our application, when translocating the robotic end-effector in its workspace, it is most intuitive to do this using the optimal, in this case shortest path which is mentally derived by observation of the objects in the robotic workspace using (higher-level) motor planning [19] [20] [21] [22] [23]. We assume that when the operator has to deviate from this mentally predefined path without receiving visual feedback in the form of a wall or something blocking our way, because invalid joint configurations do not provide visual feedback. Deriving a path to the end-effector destination will become very difficult and therefore not intuitive. When we allow the operator to stay near its mentally predefined path until it reaches the end-effector destination, we assume that the operator will define the translocation of the end-effector through the workspace as intuitive and preferable.

1) Participants: Twenty-six participants (24 male and 2 female) between 20 and 31 years old (Mean (M) = 25.77 years, Standard Deviation (SD) = 2.45) participated in the experiments. All participants had no prior experience with teleoperation in a virtual environment. In this experiment,

the independent variable is the utilized controllers for the trajectory following task. We can define two conditions: Condition 1) usage of the end-effector controller and Condition 2) usage of the novel controller. All participants will conduct in both conditions. The total number of participants will results in sufficient power for this experiment [2]. To control the carryover effects between the conditions, we use *complete counterbalancing* by letting participants undergo the various conditions in different order (Table. I) [24] [25].

subject	Training 1	Experiment 1	Training 2	Experiment 2
2k-1	Condition 1	Condition 1	Condition 2	Condition 2
2k	Condition 2	Condition 2	Condition 1	Condition 1

TABLE I: Counterbalanced sequence of the experiment for N=26 participants with $k = 1 \ldots 13$

2) Experimental design: The experiment consists of a VR environment containing a straight trajectory. This straight trajectory is the shortest path from the initial end-effector position in the front of the workspace to the back of the workspace. The trajectory will, when tracked from initial end-effector position (green sphere) to the end position (red sphere), induce a joint limit in R4 and/or in R6 (Fig. 6 for end-effector control, and Fig. 7 for novel control). Due to the joint limit(s), continuing the movement over the trajectory to the back of the workspace is not possible. Participants were asked to find a solution to correct the invalid joint configuration in both conditions. So that the end position can be attained remaining as close as possible to a trajectory. In this experiment, internal singularities are not separately tested. We assume that internal singularities can be adjusted the same way as joint limits. This is because both invalid configurations can be resolved by adjusting the joint configurations using the null-space of the robot arm. Because of the great variety in possible solutions to adjust the invalid joint configuration using the null-space controller and because not all joint groups were able to solve the invalid configurations effectively. Participants are only able to alter the configuration of the robot in the null-space using joint group 1 (i.e. R1, R2, and R3).

3) Experimental procedure: The experimental procedure is given by the flowchart in Fig. 4. In line with the (complete) counterbalancing between conditions, every even-numbered participant firstly underwent Condition 2 and then Condition 1. This order was interchanged for all uneven participants (denoted as "counterbalance" in Fig. 4). Prior to the two conditions, 4 training trials were performed. These training trials were used for the participant to ask questions and to train the participant so that low variability in performance was attained in the experimental trials. After the training session, the participant performed three experimental trials alone. The trajectory used in the training trials was the same as used in the experimental trials. After the experiment, a questionnaire assessing participant thoughts and opinions
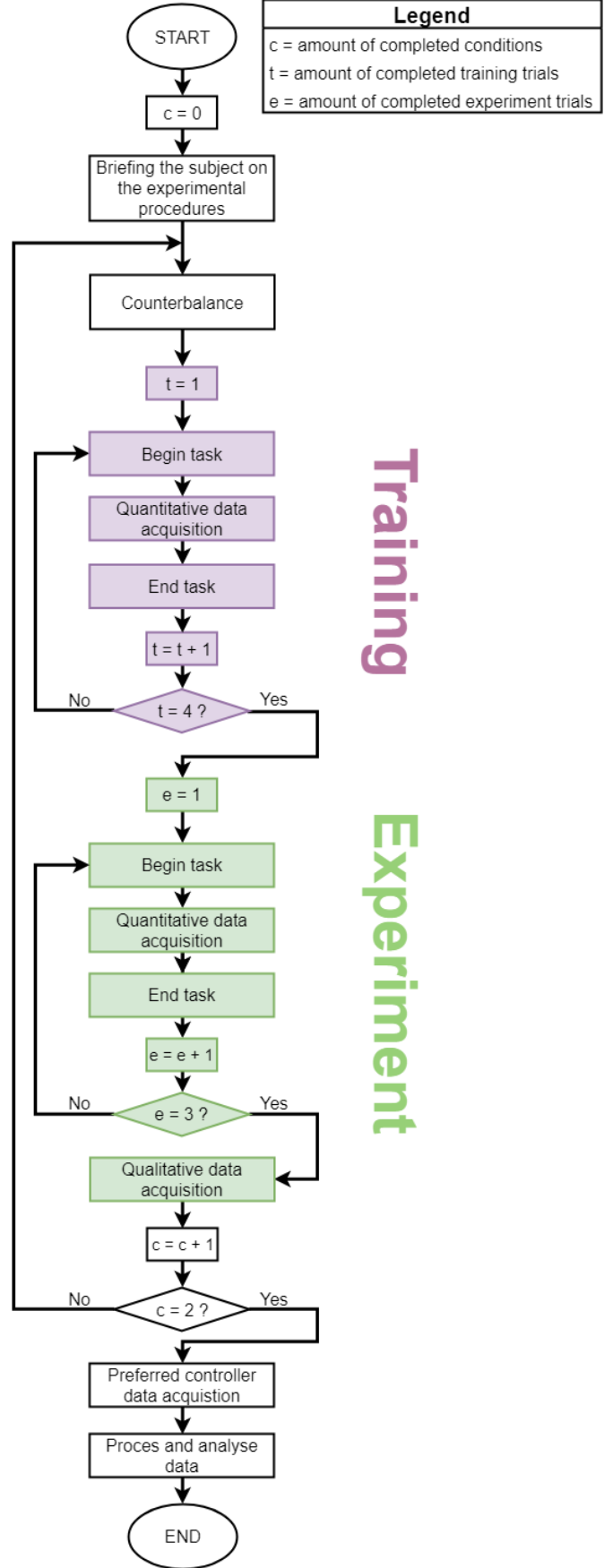

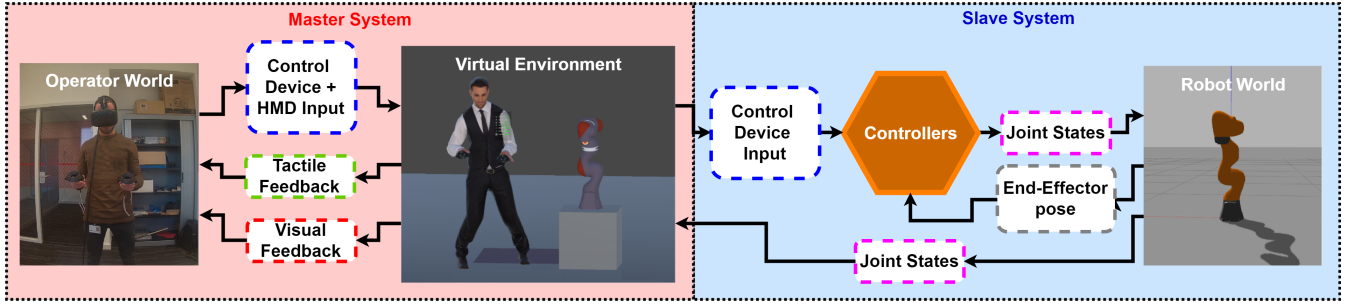Fig. 4: Experimental flowchart for the trajectory tracking task

Fig. 5: Framework as implemented in this study. The framework consists of a master system containing an HTC Vive system and a VR environment and a slave system containing two controllers and one virtual robot arm.
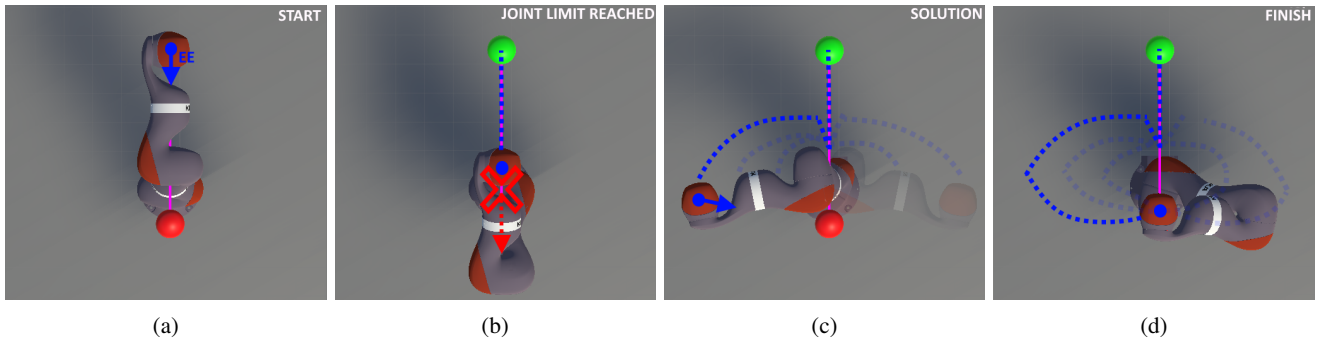

Fig. 6: The experiment using end-effector control is separated in four consecutive steps with (a) the START configuration, (b) the configuration containing a JOINT LIMIT, (c) a possible SOLUTION to avoid the joint limit and (d) the finish configuration.
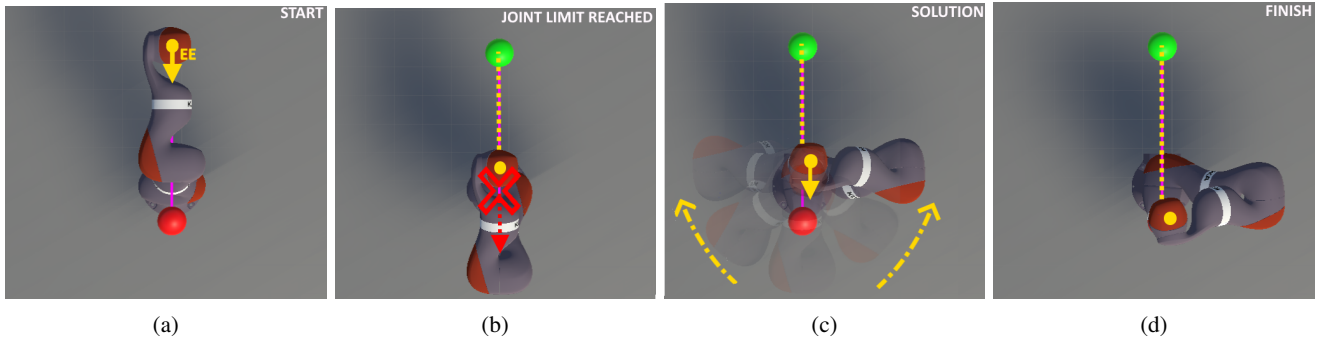

Fig. 7: The experiment using novel control is separated in four consecutive steps with (a) the START configuration, (b) the configuration containing a JOINT LIMIT, (c) a possible SOLUTION to avoid the joint limit and (d) the finish configuration.

about both controllers was answered. When both conditions were completed, the participant was asked to specify its preferred controller.

4) Task Performance Metrics: To analyze the participant's task performance we utilize three metrics. These metrics are:

a) Accuracy: Trajectory Accuracy (TA) is defined as the mean maximum absolute trajectory error of the end-effector barycentre with respect to the predefined trajectory over the experimental trails. The end-effector barycentre is the line which coordinates $\bar{x}_i$, $\bar{y}_i$ and $\bar{z}_i$ are the mean coordinates of a cluster of n points intersecting the i-the normal plane. x_{ti}, y_{ti} and z_{ti} are the coordinates of the i-th point on the predefined trajectory. This line denotes the mean path of the end-effector from the initial position to the final position. In this experiment $i = 1 \ldots 30$.

$$TA = max\sqrt{(\bar{x}_i - x_{ti})^2 + (\bar{y}_i - y_{ti})^2 + (\bar{z}_i - z_{ti})^2} \quad (15)$$

b) Completion time: Trajectory Completion Time denotes the mean time in seconds over the experimental trials, to move the end-effector from the begin position to the end position.

c) Effort: The effort is quantified as the mean amount of absolute work done on the right control device over two consecutive points Δs in the experimental trials as shown in (16). Here, m is the mass of the right control device. Δt is the

8

sampling time rate. Δv and Δs are respectively the difference over the velocity and the position of the right control device. Velocity and position data are read directly from the right control device. Due to the high Δt, the covered path Δs is considered to be a straight line with constant force F. This results in (16) to be a valid approach to calculate the effort in terms of work W.

$$W = F \cdot \Delta s = m \cdot a \cdot \Delta s = m \cdot \frac{\Delta v}{\Delta t} \cdot \Delta s \qquad (16)$$

5) Subjective Metrics: To analyze participant thoughts and opinions, the van der Laan Questionnaire [26] is used. The van der Laan Questionnaire assesses the user acceptance of both controllers that are presented in this study. The questionnaire consists of nine 5-point rating scales. These scales designate the usefulness and user satisfaction of the system. Usefulness reflects the practical aspects of the controller in accomplishing the trajectory following task. Satisfaction indicates the fulfillment of one's wishes, expectations, needs, or the pleasure derived from this [26].

To quantify and conclude the thoughts and opinions of the participants about the controllers, a final question will be asked to asses the user preferred controller. This question will result in a binary result of the preferred controller per participant.

6) Hypotheses: It is hypothesized that for $p = 0.05$: 1) the novel controller will have a significantly lower error or significantly higher trajectory accuracy in the trajectory following task than the end-effector controller. 2) The novel control controller will have a trajectory completion time equal to the trajectory completion time of the end-effector controller. 3) Operators using the novel controller will use significantly less effort when operating the robot arm than operators using the end-effector controller. 4) The novel controller will have a significantly higher usefulness rating than the end-effector controller. 5) The novel controller will have a significantly higher satisfaction rating than the end-effector controller.

7) Statistical Analysis: For the task performance metrics, the performance of all participants is analyzed by calculating the mean over the experimental trials. All participants qualitative and subjective data will be divided into two groups. These groups are an end-effector controller group containing all participant condition 1 data and a novel controller group containing all participant condition 2 data. For the evaluated metrics, we assume no homogeneity in the variance and no normality of the data in both conditions. To test the normality of the data we use the Shapiro-Wilk and Shapiro-Francia normality test [27] [28], testing the null hypothesis which states that the data sample comes from a normally distributed population for $p = 0.05$. To evaluate homogeneity in variance we use Levene's test [27] [29]. The test of Levene tests the null hypothesis which states that the population variances of

both conditions are equal (homogeneous) for $p = 0.05$. For the statistical analysis of the quantitative and subjective data, in line with the hypotheses and our assumptions we use the Wilcoxon signed-rank test instead of the paired Student t-test [27]. Utilizing the one-tailed Wilcoxon signed ranked test to evaluate the difference in means of both groups for the metrics: accuracy, effort, usefulness, and satisfaction. Trajectory completion time is evaluated using the two-tailed Wilcoxon signed-rank test. The difference in user controller preference is not statistically tested. Analysis of the data is performed using MATLAB R2017a [30].

III. RESULTS

Fig. 8 shows the results of the generated quantitative task performance and subjective data of the end-effector (EE) and novel (NV) control groups from the within-subject design experiment. Fig. 9 shows the raw trajectory barycentre data of all participants in both groups preforming the trajectory following task. The group statistics, data of the statistical tests and user preference data are respectively tabulated in Table. II, III and IV. Of the 26 participants, only 24 participants filled in the van der Laan questionnaire.

Table. III shows that the distribution of the trajectory accuracy (end-effector group) data and effort data is significantly different from a normal distribution. Whereas the data distribution of the metrics accuracy (novel controller group), time, usefulness and satisfaction did not significantly deviate from normal distribution. As for the homogeneity in variance between the conditions, all metric data showed a significant difference in homogeneity between variances of both conditions.

The raw trajectory barycentre data in Fig. 9 shows that when participants using end-effector control reach the back of the workspace (middle of the trajectory), they deviate from the predefined trajectory. Participants utilizing the novel controller, move in a near straight path back of the workspace, having a near constant error with the predefined trajectory.
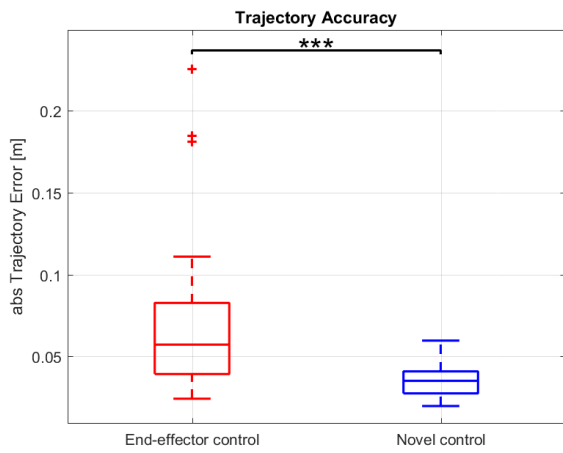
A. Accuracy

Evaluation of the results in trajectory accuracy showed a significant lower trajectory error for participants using the novel controller than participants using the end-effector controller (Fig. 8a).
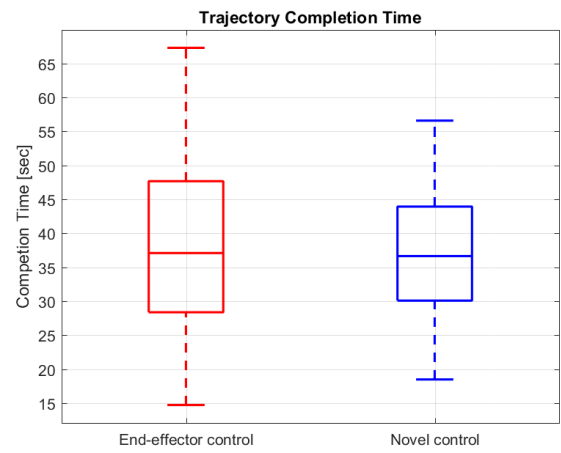
B. Completion Time

Results in trajectory completion time between the end-effector controller group and the novel controller group resulted in no significant differences between the groups (Fig. 8b).
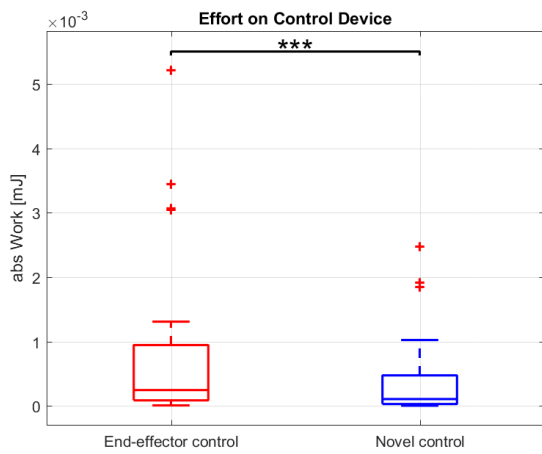
C. Effort

For the end-effector control group, the effort on the control device was significantly higher than the novel controller group for the trajectory tracking task (Fig. 8c). The effort data visualized in Fig. 8c alone fails to explain the difference
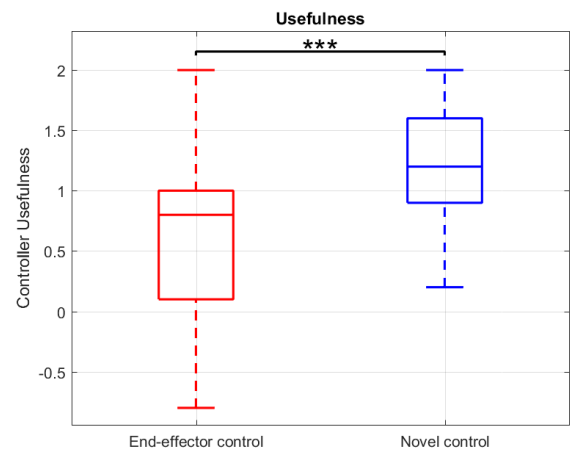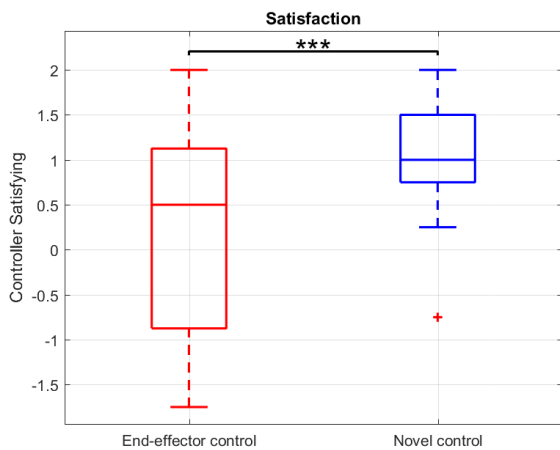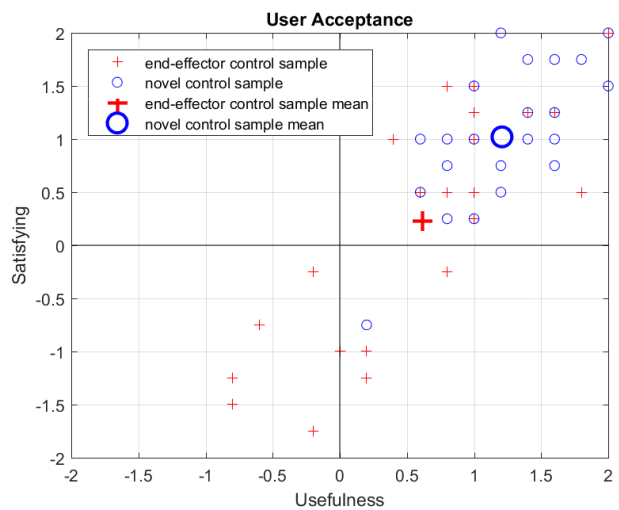
9

Fig. 8: Task performance metric data in boxplots of the groups for (a) accuracy ($p < .001$), (b) completion time ($p = .9292$) and (c) effort ($p < .001$). Subjective metric data of the groups for (d) usefulness ($p < .001$), (e) satisfaction ($p < .001$) in boxplots and (f) user acceptance in a user acceptance graph

TABLE II: Table containing the Group Statistics of both the end-effector and novel controller group for all statistically analyzed metrics.

Group Statistics

Metric		Controller Group	Sample Size (N)	Median (Mdn)	Mean (M)	Standard Deviation (SD)
Accuracy	Mean Max Abs Trajectory Error (m)	EE	26	.0572	.0721	.0515
		NV	26	.0351	.0356	.0101
Time	Mean Trajectory Completion Time (sec)	EE	26	37.09	38.77	14.72
		NV	26	36.65	37.40	9.59
Effort	Mean Work on the Control Device (J)	EE	26	.25e-06	.90e-06	1.30e-06
		NV	26	.11e-06	.39e-06	.67e-06
Usefulness	vd Laan	EE	24	.80	.62	.77
		NV	24	1.20	1.21	.46
Satisfaction	vd Laan	EE	24	.50	.23	1.09
		NV	24	1.00	1.02	.63

TABLE III: Table containing all the results of the Shapiro-Wilk and Shapiro-Francia (SW/SF) normality tests, the Levene's test for homogeneity in variance and the Wilcoxon signed-ranked tests.

Dependent/Paired Samples Test

Metric		Controller Group	SW/SF normality test p-value	SW-statistic	Levene's homogeneity test p-value	F-statistic	Wilcoxon signed ranked test T-statistic	p-value	z-value	Effect size r
Accuracy	Mean Max Abs Trajectory Error (m)	EE	p<.001	.7615	p<.001	15.8562	327	p<.001	3.8351	0.5318
		NV	p=.5127	.9656						
Time	Mean Trajectory Completion Time (sec)	EE	p=.6195	.9699	p=.0321	4.8597	172	p=.9292	-0.0889	-0.0123
		NV	p=.9467	.9841						
Effort	Mean Abs Work on Control Device (J)	EE	p<.001	.6812	p=.0277	5.1428	318	p<.001	3.6065	0.5001
		NV	p<.001	.6163						
Usefulness	vd Laan	EE	p=.2893	.9513	p=0.0198	5.8254	28	p<.001	-3.3411	-0.4822
		NV	p=.7760	.9744						
Satisfaction	vd Laan	EE	p=.1123	.9327	p=0.0022	10.4932	24	p<.001	-3.3242	-0.4798
		NV	p=.1194	.9360						

TABLE IV: Table containing the controller preference of all participants

User Controller Preference

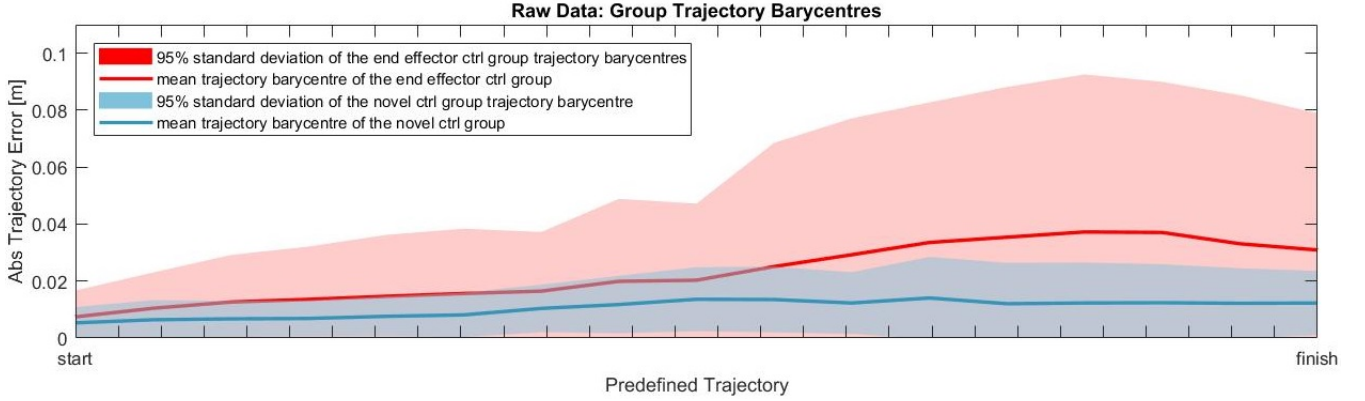|	Controller Group	
Metric	EE	NV
User Preferred Controller (%)	19 (5/26)	81 (21/26)

Fig. 9: The Raw trajectory data of all participants in the end-effector and novel controller groups projected on the XY-plane.
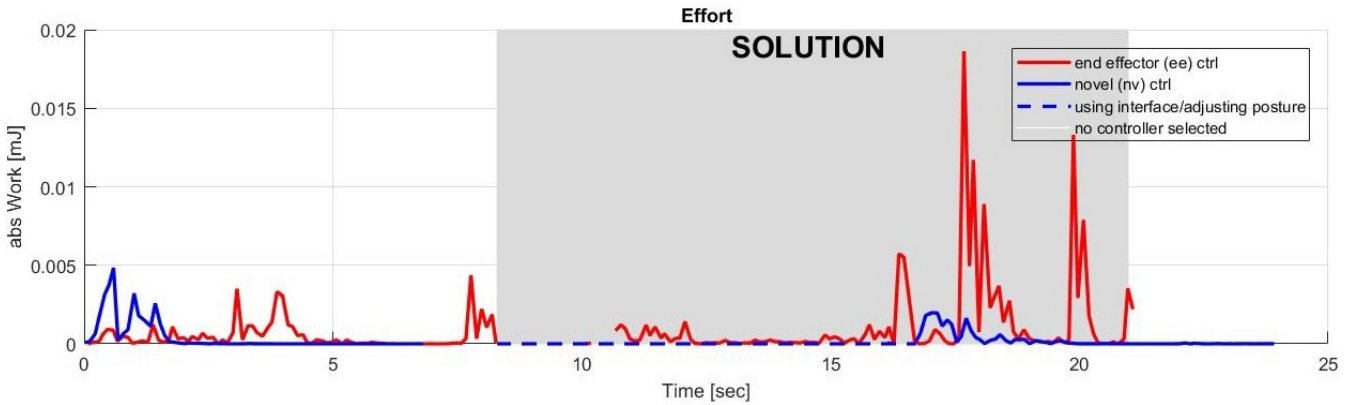

Fig. 10

Fig. 11: The effort in work [J] on the control device for the total trajectory tracking task for the end-effector control group and the novel control group. Where the grey area indicates the work done on the right control device in the SOLUTION part of the experiment (Fig. 6c and Fig. 7c).

between the usage of the end-effector controller and the novel controller. To clarify this difference we use a work (W) versus time data graph (Fig. 10). This graph shows the data of subject 20 ($\mu = .91\ \mu J$) representing the end-effector controller group and subject 7 ($\mu = .32\ \mu J$) representing the novel controller group. Using Fig. 10, if we focus on the SOLUTION (grey) part (associated with the part of the experiment visualized in Fig. 7c and Fig. 6c), we can see that when using the end-effector controller, the work on the right control device is significantly higher and less smooth the when using the novel controller.

D. User Acceptance

End-effector control was rated significantly lower for usefulness (Fig 8d) and satisfaction (Fig. 8e) than the novel controller. Fig. 8f visualizes this significant effect using a user acceptance (e.g. usefulness versus satisfaction) graph.

E. User Preference

The concluding question quantifying the preferably of both controllers resulted in 81% of the participants preferring the

novel controller over the end-effector controller. 19% of the participants preferred the end-effector controller over the novel controller for the given task.

IV. DISCUSSION

A. Main results

In this study, we aimed to develop and validate a novel controller used for free-air movement applications to realize total and intuitive workspace utilization. The validation was done using a within-subject design experiment, assessing operator performance, acceptance and controller preference when operating the robot arm. The performance was measured using quantitative task performance metrics: accuracy (error), completion time and effort. User acceptance and preference were analyzed using subjective metrics: usefulness, satisfaction and user controller preference.

Using Shapiro-Wilks and Levene's test we showed that the captured data is either not homogeneous in variance or both not homogeneous in variance and not normal distributed.

Where both the paired Student t-test and the Wilcoxon signed-rank test were candidates to be used to evaluate both groups by their mean values. The Wilcoxon signed-rank test resulted to be a better candidate because the data did not meet the assumptions and requirements required for the paired Student t-test [27].

1) Accuracy: It was hypothesized that the novel controller will have significantly higher accuracy than the end-effector controller. Consistent with the hypothesis, Fig. 8a shows that the novel controller significantly outperforms the end-effector controller in trajectory following accuracy. This difference can be explained by assessing the working principle of both controllers. The end-effector controller grants the operator only the possibility to directly control the pose of the end-effector. The joint configuration of the robot can only be indirectly corrected. The novel controller grants the possibility to (directly) adjust the joint configuration of the robot with respect to its base with a fixed end-effector position. Now instead of moving the end-effector to change the joint configuration of the robot, the joint configuration is directly manipulated. This results in the adjustment of the invalid joint configuration by which we attain higher trajectory tracking accuracy when using the novel controller. Enabling us to remain near the (mentally) predefined path when moving through the workspace.

2) Completion Time: Fig. 8b shows approximately equal mean completion times for the novel controller group and the end-effector group. This insignificance difference is consistent with the hypothesis and can be explained due to the additional joint adjusting steps (e.g. joint selection and adjustment) taken when using the novel controller. The insignificance in the completion time indicates that the additional steps required to find a joint limit avoiding solution using novel control are approximately equal to the time used when finding a solution using end-effector control. The insignificance in the completion time is a design choice. To speed up the novel controller we could have chosen a faster control switching design. The interface was preferred because the novel controller is developed to adjust the invalid joint configuration with the use of all seven joints in future applications.

3) Effort: In line with our hypothesis, we prove that to control the robot arm, the novel controller group uses significantly less effort than the end-effector group (Fig. 8c). Low effort indicates smooth and constant motion of the control device resulting in effortless control of the robot arm. High fluctuation rates and high values in effort indicate a "searching" behavior of the operator. The operator uses several movements to work around the joint-limits. Because joint limits result in the robot terminating its movements, the operator tries to force the robot through its joint limit by applying more force on the control device. More force will result in an acceleration of the control device, resulting

in a peak in the applied effort. When a solution is found the applied effort declines until the end position is reached. This "searching" behavior cannot be found when using the novel controller. Because when using the novel controller the adjustment of the joint configuration results in the robot not attaining new joint limits. Due to this, the operator can operate the end-effector with approximately constant velocity to the destination.

4) User Acceptance: For the novel controller, we hypothesized that user acceptance consisting out of usefulness and satisfaction would be rated significantly higher than the end-effector controller. Consistent with our hypotheses, we showed that the user acceptance for the novel controller was indeed rated significantly higher (Fig. 8). For the novel controller, all participants rated the usefulness of the novel controller positive. All participants except one rated the novel controller as satisfying (positive value). Higher acceptance indicates that in a situation where the novel controller is provided, the user will enable the controller for a trajectory following task. High acceptance also indicates a productive investment of effort in designing and building this novel controller [26].

5) User Preference: The final question quantifying the preference for both controllers resulted in a large proportion of the group (81%) preferring the novel controller over the end-effector controller. For all metrics except the trajectory tracking completion time, the results show a significant difference in performance and user acceptance in favor of the novel controller. According to these results, preferring the novel controller over the end-effector controller is a obvious result. Because we evaluate the means of the groups, results of participants who perform better with the end-effector controller and/or rate the end-effector higher than the novel controller are blended in the total data sample of the group. If we assume that high performance and/or higher user acceptance leads to a participant preferring a certain controller. Using the user controller preference metric we can see that not every participant performed better with the novel controller as the results indicate. The results indicate that a large proportion of the group preformed better using the novel controller but fails to conclude anything about the participants who did not. Because of this, the results should be used and evaluated with caution.

Similar to the studies of [4], [7] and, [8] we showed that the usage of the null-space projection control is beneficial in adjusting invalid joint configurations. In this study, we demonstrated that next to (semi-)autonomous applications, null-space projection control is also beneficial for VR mediated teleoperation free-air movement applications. In addition to the study of [2], we proved that accurate and intuitive operation is also possible in sections of the workspace where invalid joint configurations are attained.

B. Limitations

1) Individual differences: The statistical effect in trajectory tracking accuracy between the two controller groups was lower than expected. A group of participants was able to indirectly rotate the joint configuration of the robot around its base for near constant end-effector position using end-effector control. Resulting in approximately equal performance as when using the novel controller. The remainder of the participants were not able to indirectly adjust the configuration of the robot resulting in the deviation of the trajectory and a high trajectory error. This individual difference resulted in a lower statistical effect and higher variability for trajectory accuracy and effort than hypothesized.

2) Uneven gender distribution in samples: In this study, we analyzed 24 male and 2 female students in robotic arm operation performance, acceptance and preference. The distribution of the participants results in gender imbalance in the groups. Next to being all students, this imbalance lowers representation of this study for the full population and so the statistical power [31]. Due to practical considerations regarding the time and expense required to achieve gender-balanced samples, the current samples were used.

V. CONCLUSION AND RECOMMENDATIONS

In free-air movement applications, joint limits and singularities limit the movements of robotic arms and thereby the total and intuitive utilization of the robotic workspace. Our goal was to develop and validate a novel controller for VR mediated teleoperation of the KUKA LBR iiwa 7 robot arm using the null-space of the robot. To adjust invalid configurations to valid configurations. Enabling intuitive utilization of the total workspace. Validation was done using a within-subjects design experiment testing the novel controller against the state-of-the-art end-effector controller using 26 participants having no operating experience. The participants had the task to track a straight trajectory from the front to the back of the workspace as accurate as possible. This trajectory is assumed to mimic the shortest and most intuitive path mentally derived when having to move from the end-effector initial position to a destination in the back of the workspace. Tracking the trajectory will induce an invalid configuration, terminating the movement of the robot. Resulting in the end-effector having to deviate from the predefined trajectory inducing difficult and not intuitive operation. The experiment evaluated participant performance, acceptance and controller preference in adjusting the invalid configuration using both controllers to eventually reach the back of the workspace. Results showed that the novel controller was significantly better in adjusting invalid configurations than the end-effector controller. Resulting in accurate and effortless control when moving the end-effector to the back of the workspace. The novel controller was also significantly more acceptable than the end-effector controller in usefulness and satisfaction. High user acceptance results in the novel controller being enabled for a trajectory following task instead of being shut off.

Future studies should: Firstly, evaluate the application of the remaining joint groups in free-air movement applications or other applications to determine their effect. Secondly, test larger groups to validate our results and assumptions. Finally, do (qualitative) research to explain why participants prefer a certain controller.

REFERENCES

[1] N. Hoeba, N. van der Stap, and D. Abbink, "Report: Internship tno," Master's thesis, 2018.

[2] D. B. van der Merwe and N. van der Stap, "Human-robot interaction during vr mediated teleoperation: How environment information affects spatial task performance and operator situation awareness," Master's thesis, 2018.

[3] P. K. Allen, "Cs 4733 class notes: Kinematic singularities and jacobians," Aug 2015. [Online]. Available: http://www.cs.columbia.edu/ allen/F15/NOTES/

[4] M. Hayakawa, K. Hara, D. Sato, A. Konno, and M. Uchiyama, "Singularity avoidance by inputting angular velocity to a redundant axis during cooperative control of a teleoperated dual-arm robot," in *2008 IEEE International Conference on Robotics and Automation*. IEEE, 2008, pp. 2013–2018.

[5] N. Hoeba, "Anthropomorhism in the teleoperation of robot arms," Master's thesis, Delft University of Technology, 2018.

[6] "Telerobotics enhancing robotic sensing and situational awareness for telerobotics." [Online]. Available: https://i-botics.com/

[7] H. Han and J. Park, "Robot control near singularity and joint limit using a continuous task transition algorithm," *International Journal of Advanced Robotic Systems*, vol. 10, no. 10, p. 346, 2013.

[8] L. Huo and L. Baron, "The joint-limits and singularity avoidance in robotic welding," *Industrial Robot: An International Journal*, vol. 35, no. 5, pp. 456–464, 2008.

[9] J. Van Kasteren, "Paardrijden op de snelweg," 2016. [Online]. Available: https://www.nrc.nl/nieuws/2016/07/01/paardrijden-op-de-snelweg-3015262-a1504807

[10] F. Flemisch, D. Abbink, M. Itoh, M.-P. Pacaux-Lemoine, and G. Weßel, "Shared control is the sharp end of cooperation: Towards a common framework of joint action, shared control and human machine cooperation," *IFAC-PapersOnLine*, vol. 49, no. 19, pp. 72–77, 2016.

[11] Y.-C. Liu and N. Chopra, "Control of semi-autonomous teleoperation system with time delays," *Automatica*, vol. 49, no. 6, pp. 1553–1565, 2013.

[12] J. Rubi, A. Rubio, and A. Avello, "Involving the operator in a singularity avoidance strategy for a redundant slave manipulator in a teleoperated application," in *IEEE/RSJ International Conference on Intelligent Robots and Systems*, vol. 3. IEEE, 2002, pp. 2973–2978.

[13] B. P. DeJong, J. E. Colgate, and M. A. Peshkin, "Improving teleoperation: reducing mental rotations and translations," in *Robotics and Automation, 2004. Proceedings. ICRA'04. 2004 IEEE International Conference on*, vol. 4. IEEE, 2004, pp. 3708–3714.

[14] "Use the world's best virtual reality technology, royalty free." [Online]. Available: https://partner.steamgames.com/vrlicensing

[15] [Online]. Available: http://www.root-motion.com/final-ik.html

[16] TullyFoote, "Ros kinetic." [Online]. Available: http://wiki.ros.org/kinetic

[17] davetcoleman, "Gazebo." [Online]. Available: http://wiki.ros.org/gazebo_ros_pkgs

[18] D. E. Whitney, "Resolved motion rate control of manipulators and human prostheses," *IEEE Transactions on man-machine systems*, vol. 10, no. 2, pp. 47–53, 1969.

[19] P. Morasso, "Spatial control of arm movements," *Experimental brain research*, vol. 42, no. 2, pp. 223–227, 1981.

[20] W. Abend, E. Bizzi, and P. Morasso, "Human arm trajectory formation." *Brain: a journal of neurology*, vol. 105, no. Pt 2, pp. 331–348, 1982.

[21] Y. Uno, M. Kawato, and R. Suzuki, "Formation and control of optimal trajectory in human multijoint arm movement," *Biological cybernetics*, vol. 61, no. 2, pp. 89–101, 1989.

[22] A. L. Wong, A. M. Haith, and J. W. Krakauer, "Motor planning," *The Neuroscientist*, vol. 21, no. 4, pp. 385–398, 2015.

[23] Y. M. Marghi, F. Towhidkhah, and S. Gharibzadeh, "Human brain function in path planning: a task study," *Cognitive Computation*, vol. 9, no. 1, pp. 136–149, 2017.

[24] J. C. De Winter and D. Dodou, *Human Subject Research for Engineers: A Practical Guide*.   Springer, 2017.

[25] B. J. Underwood, "Experimental psychology: An introduction." 1949.

[26] J. D. Van Der Laan, A. Heino, and D. De Waard, "A simple procedure for the assessment of acceptance of advanced transport telematics," *Transportation Research Part C: Emerging Technologies*, vol. 5, no. 1, pp. 1–10, 1997.

[27] A. Field, *Discovering statistics using IBM SPSS statistics*.   sage, 2013.

[28] A. BenSada, "Shapiro-wilk and shapiro-francia normality tests. - file exchange - matlab central." [Online]. Available: https://nl.mathworks.com/matlabcentral/fileexchange/13964-shapiro-wilk-and-shapiro-francia-normality-tests

[29] A. Schurger, "Levene's test for homogeneity of variance - file exchange - matlab central." [Online]. Available: https://nl.mathworks.com/matlabcentral/fileexchange/44415-levene-s-test-for-homogeneity-of-variance

[30] *MATLAB version 9.2.0.556344 (R2017a)*, The Mathworks, Inc., Natick, Massachusetts, 2017.

[31] E. R. Dickinson, J. L. Adelson, and J. Owen, "Gender balance, representativeness, and statistical power in sexuality research using undergraduate student samples," *Archives of Sexual Behavior*, vol. 41, no. 2, pp. 325–327, 2012.

A

EXTENSIVE INFORMATION: HUMAN SUBJECT EXPERIMENT METRICS

A.1. TRAJECTORY ACCURACY

Appendix A.1 will give additional information about the metric: *Trajectory Accuracy*. The metric *Trajectory Accuracy* is quantified as the mean maximum absolute trajectory error of the end-effector barycentre along the predefined trajectory over the experiment trials. The metric is an adaptation of the metric used in [2] to determine the *Positioning path accuracy (ATp)*.

Next to the maximum absolute error of the end-effector barycentre, we could also have used the maximum error or the mean error of the end-effector path along the predefined trajectory to quantify the *Trajectory Accuracy*. The paragraph below explains why we did not use these values.

The maximum error value of the end-effector path is unable to fully evaluate the accuracy of the whole end-effector path because it only uses one (maximum value) sample in time and space. The mean error of the end-effector path value is unable to quantify the difference between the novel and the end-effector controller. This is because, for both controllers, the end-effector path is the same for a large part of the trajectory. Resulting in small deviations of the mean values for both controllers. We use the mean maximum absolute error of the end-effector barycentre along the predefined trajectory because it combines both the best properties of the mean path error and maximum path error methods.

According to this [1], "Trajectory Accuracy (TA) is defined as the mean maximum absolute trajectory error of the end-effector barycentre with respect to the predefined trajectory over the experimental trails. The end-effector barycentre is the line which coordinates $\bar{x}_i$, $\bar{y}_i$ and $\bar{z}_i$ are the mean coordinates of a cluster of n points intersecting the i-the normal plane. x_{ti}, y_{ti} and z_{ti} are the coordinates of the i-th point on the predefined trajectory. This line denotes the mean path of the end-effector from the initial position to the final position. In this experiment $i = 1 \ldots 30$.".

We will compute the end-effector barycentre using Fig.A.1,A.2,A.3,A.4, A.5 and A.6 to visualize the 6 steps needed to construct the barycentre to eventually determine the *Trajectory Accuracy* per participant.

Fig. A.1 shows a end-effector path of a participant and the "to be followed"/predefined trajectory as used in the experiment. We can see that the end-effector path is not a straight path. Due to the attained joint limits participants have to deviate from the trajectory resulting in chaotic end-effector path as visualized.
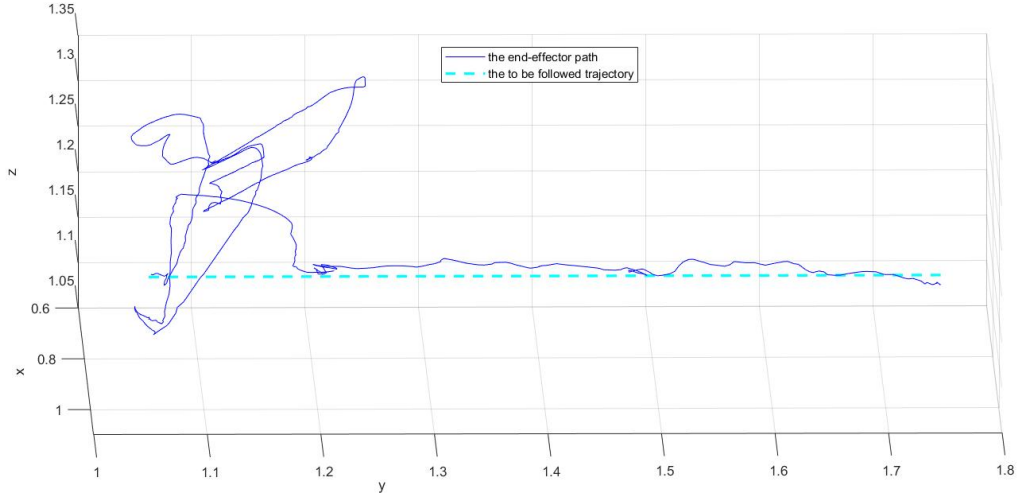
Figure A.1

We can derive the end-effector barycentre by sampling the end-effector path. We sample the total path 30 times. The sampling is facilitated by 30 normal planes (as visualized in Fig. A.2).
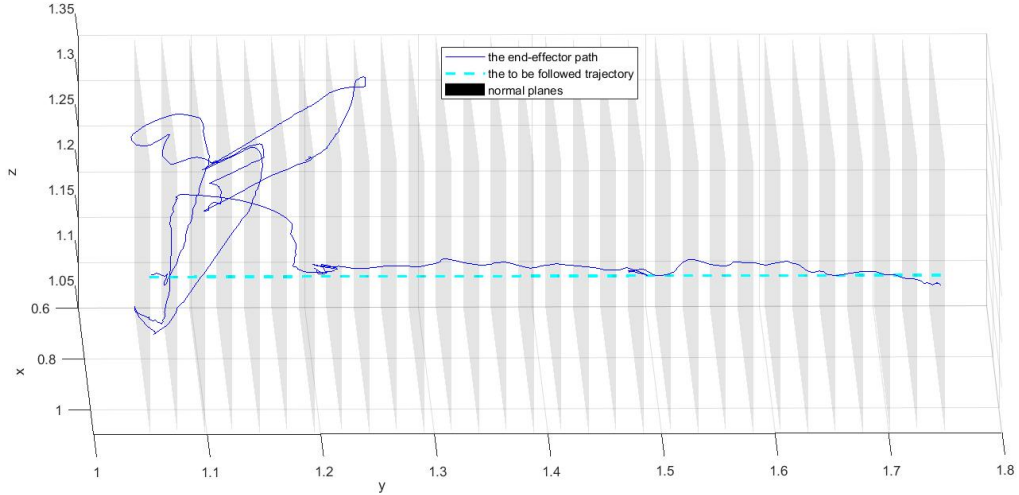

Figure A.2

Sampling of the end-effector path results in a set of values in space, which is a cluster of intersection points of the end-effector path with the i-the normal plane ($i = 1\ldots30$) (Fig. A.3). Because the trajectory itself is sampled with 100 Hz, the path itself is not continuous, but a path of connected discrete values. This results in the probability that there are no intersections of discrete end-effector path with the normal plane. To ensure that we will have at least one intersection point, we search for intersection points with a tolerance of 0.005 m on both sides of the normal plane.

Using the intersection clusters as visualized in Fig. A.3, we can now determine the coordinates $\bar{x}_i$, $\bar{y}_i$ and $\bar{z}_i$ which are the mean coordinates of a cluster of n points intersecting the i-the normal plane. These mean coordinates give us a mean end-effector position of all normal plane intersections, indicating the mean position of where the end-effector has been in that part of space.

Connecting the mean coordinates of the clusters result in the barycentre shown in Fig. A.5.

We calculate the absolute distance between the mean coordinate of the intersection cluster of the i-th normal plane ($\bar{x}_i, \bar{y}_i, \bar{z}_i$) and the i-th point on the predefined trajectory (also intersected by the i-th normal plane). To determine the maximum distance of the end-effector barycentre along the predefined trajectory as shown in
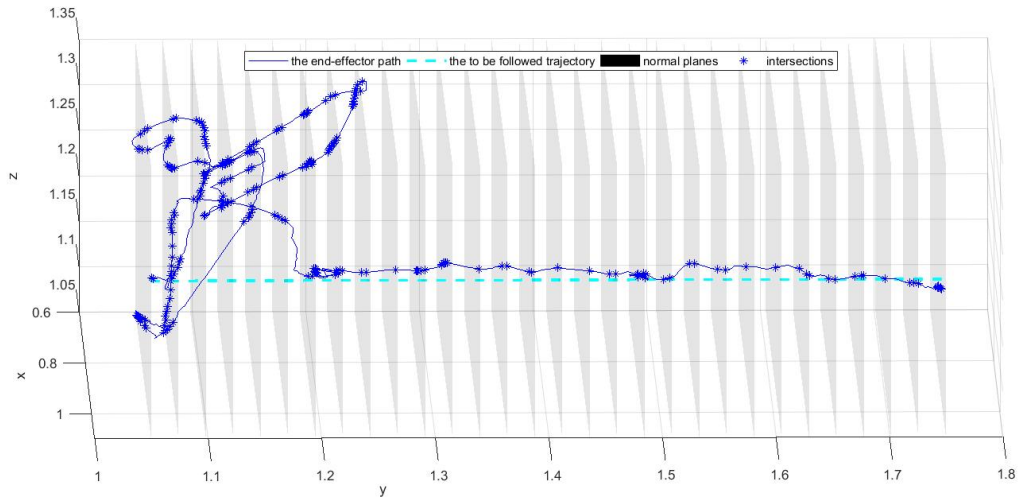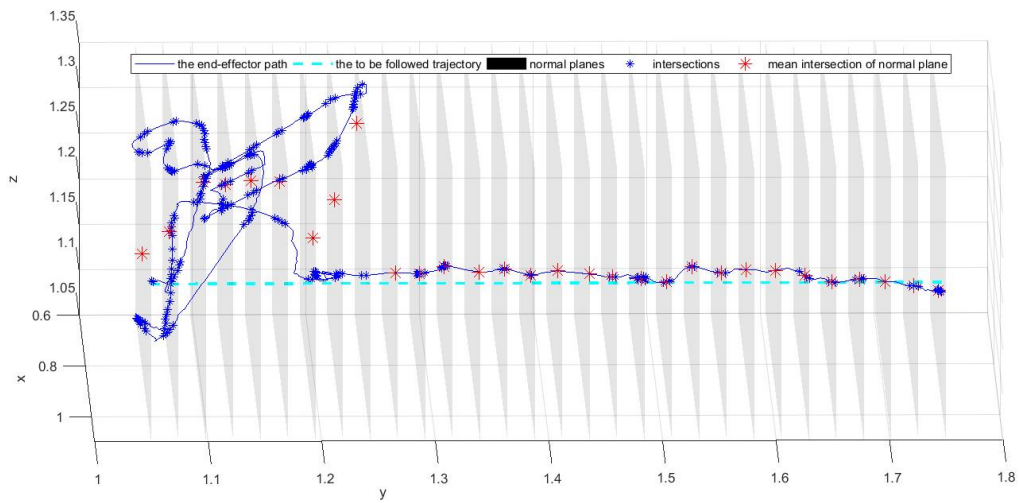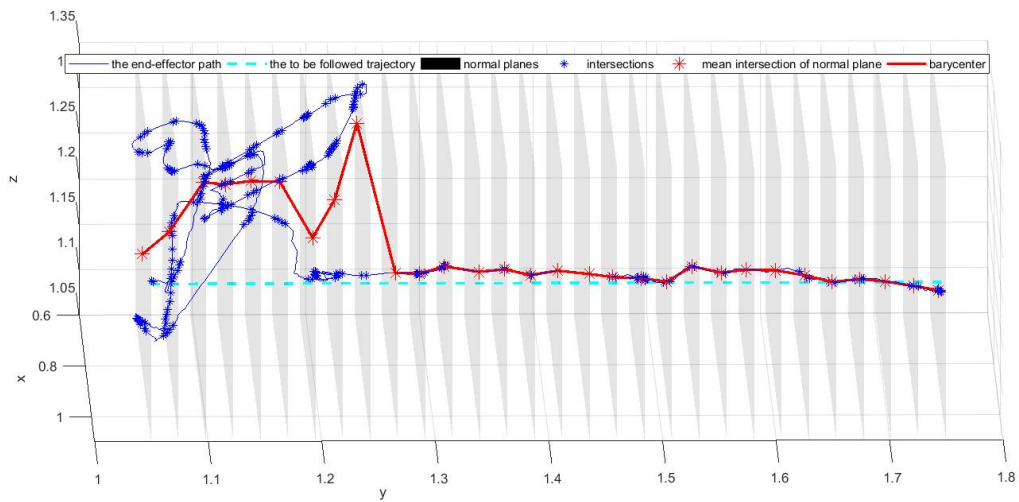
Figure A.3

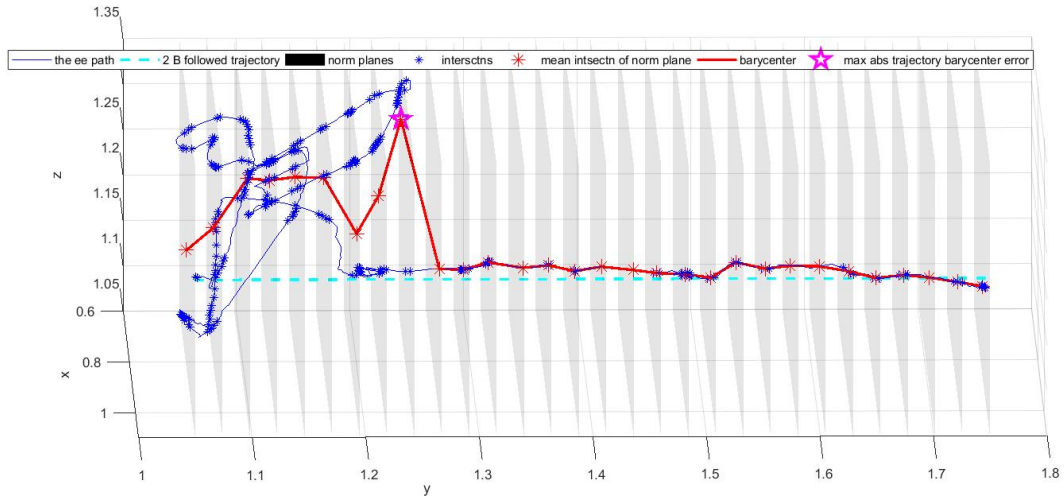
Figure A.4

Figure A.5

Eq. (A.1) (Fig. A.6).

Figure A.6

$$TA = max\sqrt{(\bar{x}_i - x_{ti})^2 + (\bar{y}_i - y_{ti})^2 + (\bar{z}_i - z_{ti})^2} \tag{A.1}$$

Finally, we derive the maximum absolute error of the end-effector barycentre along the predefined trajectory for all three experimental trails and calculate the mean value. This mean maximum absolute error value is used as the Trajectory Accuracy of a participant. In the virtual environment, Trajectory Accuracy is denoted as 1. as in Fig. A.7.

In Fig. A.6 we can see that when the end-effector trajectory moves from the begin position to the end position in a straight path, the end-effector path is equal to the end-effector barycenter. Only when certain sections of space (defined by the normal planes) are reached more than one time, the end-effector path is not equal to the end-effector trajectory barycenter.
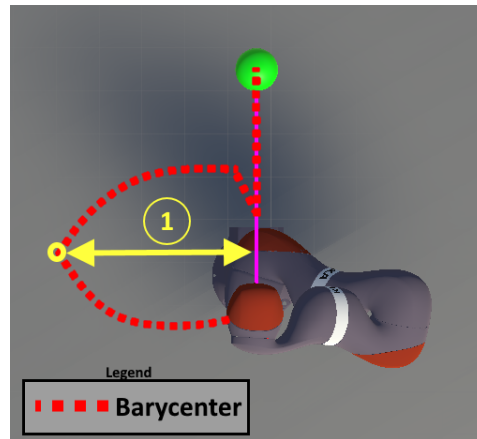

Figure A.7

A.2. Trajectory Completion Time

Appendix A.2 visualizes the metric *Trajectory Completion Time* (Fig. A.8). In Fig. A.8 we can see that the *Trajectory Completion Time* is the time needed to move from the begin position (green sphere) to the end position (red sphere) [1].
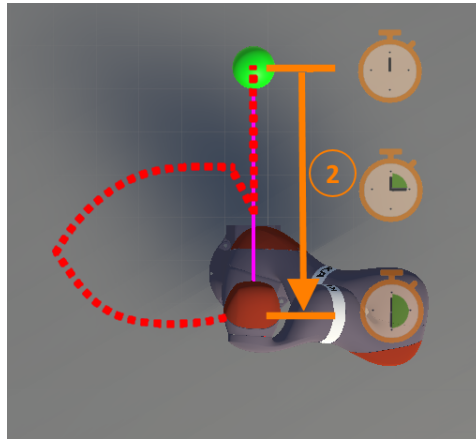
Figure A.8

A.3. EFFORT

Appendix A.3 gives supplementary information in how we quantify the metric: *Effort*. According to [1], the effort is defined as the mean absolute work on the (right hand) control device over the controlled path as shown in (A.2). As visualized in Fig. A.9 the commanded path is a path of connected discrete values. These discrete values represent the position of the control device in space for a certain value in time s_{t-n} with $n = 0 \ldots \infty$. Because we assume that the distance between to position of the control device Δs is small because we sample with a rate of 100 Hz. We assume that the commanded path between two positions is straight and that the force between both positions constant resulting in equation (??) to be a valid approach [1].

$$W = F \cdot \Delta s = m \cdot a \cdot \Delta s = m \cdot \frac{\Delta v}{\Delta t} \cdot \Delta s \tag{A.2}$$
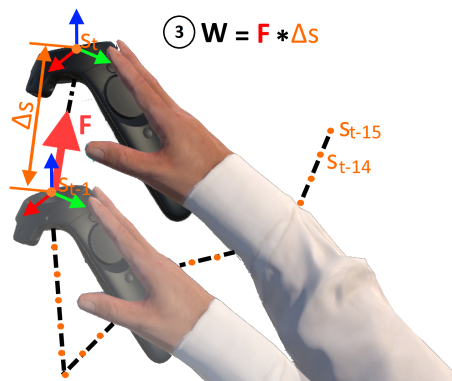
Figure A.9

REFERENCES

[1] N. Hoeba, "Vr mediated teleoperation: Total workspace utilization using null-space projection control," Master's thesis, Delft University of Technology, 2019.

[2] "Industriële robots - Prestatie-eisen en bijbehorende beproevingsmethoden," International Organization for Standardization, Geneva, CH, Standard, May 1998.

B

HUMAN SUBJECT EXPERIMENT SETUP AND SPECIFICATIONS

B.1. DEVICE SETUP AND SPECIFICATIONS

Appendix B.1 will give information about the human subject experimental setup and the specifications of the devices used for the human subjects experiments.

Fig. B.1 shows a schematic overview of the used experimental setup. All devices are labeled from 1 to 5. Information about the devices can be found in Table B.1.

Next to the schematic overview, Fig. B.2a and Fig. B.2b show the experimental setup as used in the Cognitive Robotics (CoR) lab at the TU Delft.
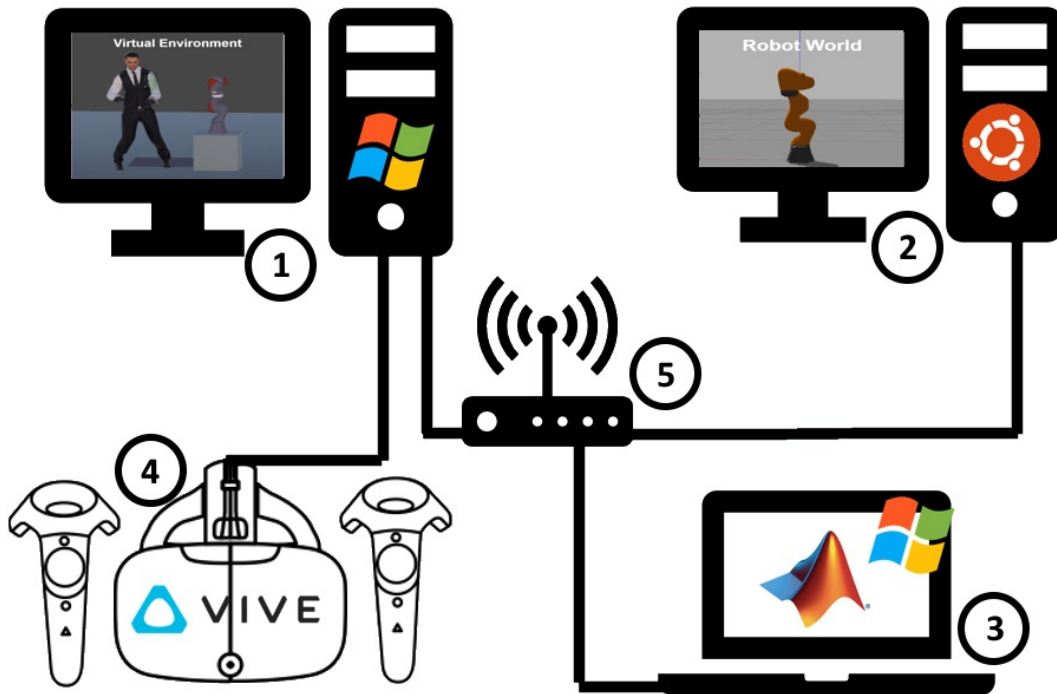
Figure B.1: A schematic overview of the experimental setup used in the human subject experiments. In this figure (1) is the master system computer, (2) is the slave system computer, (3) is a laptop collecting all the participant data, (4) is the HTC Vive VR system (HMD+Controllers) and (5) is a network splitter used to connect all computers on a single network

23

Table B.1: Table containing specifications of the devices used in the human subject experiments labeled from 1 to 5.

|	Item Number				
	1	2	3	4	5
Device	Desktop	Desktop	Laptop	VR system	Network switch
Name	Alienware Aurora R6	HP Z210 Workstation	HP ZBook Studio G5	HTC Vive	NETGEAR GS605 5-Port Gigabit Desktop Switch
OS type	Microsoft Windows 10 Enterprise	Ubuntu 16.04 LTS	Microsoft Windows 10 Home	SteamVR (Win/Linux/MacOS)	
RAM	16 GB	3,8 GiB	16 GB		
Processor	Intel(R) Core(TM) i5-7400 CPU @ 3.00GHz, 3000 Mhz, 4 Core(s), 4 Logical Processor(s)	Intel(R) Core(TM) i5-2400 CPU @ 3.10 GHz x 4	Intel(R) Core(TM) i7-8750H CPU @ 2.20GHz		
Graphics	NVIDIA GeForce GTX 1070	AMD REDWOOD (DRM 2.50.0 /4.15.0-54-generic, LLVM 6.0.0)	Intel(R) UHD Graphics 630		
Memory	465 GB	245 GB	455 GB		
Refresh rate				90 Hz	

B.2. REMOTE DESKTOP ACCES (RDA)

Remote Data Access (RDA) a flexible infrastructure for real-time distributed data access and data acquisition created by Gert van Antwerpen and Kees van den Berg (TNO). The infrastructure, created to overcome the problem of real-time data acquisition, loosely couples between real-time and non-real time parts of data acquisition tasks, using a combination of TCP/IP network connection and shared memory resulting in a data acquisition independent of the computer architecture [3].

The RDA connection is utilized to exchange data between the slave system and the master system (i.e remote data access). Remote data access is enabled by the creation of an RDA module on the RDA server. This module stores the variables written to it. Both the slave and master system can access these variables real-time, to exchange data as being one system. In our framework, the RDA module and server are hosted by the master system.

(a)   (b)

Figure B.2: The experimental setup as used in the Cognitive Robotics (CoR) lab at the TU Delft

REFERENCES

[3] G. van Antwerpen and K. van den Berg, "Remote Data Access a flexible infrastructure for real0tim distributed data access and data acquistion," 2014.

C

HUMAN SUBJECT EXPERIMENT DATA CAPTURE

C.1. MATLAB INTERFACE
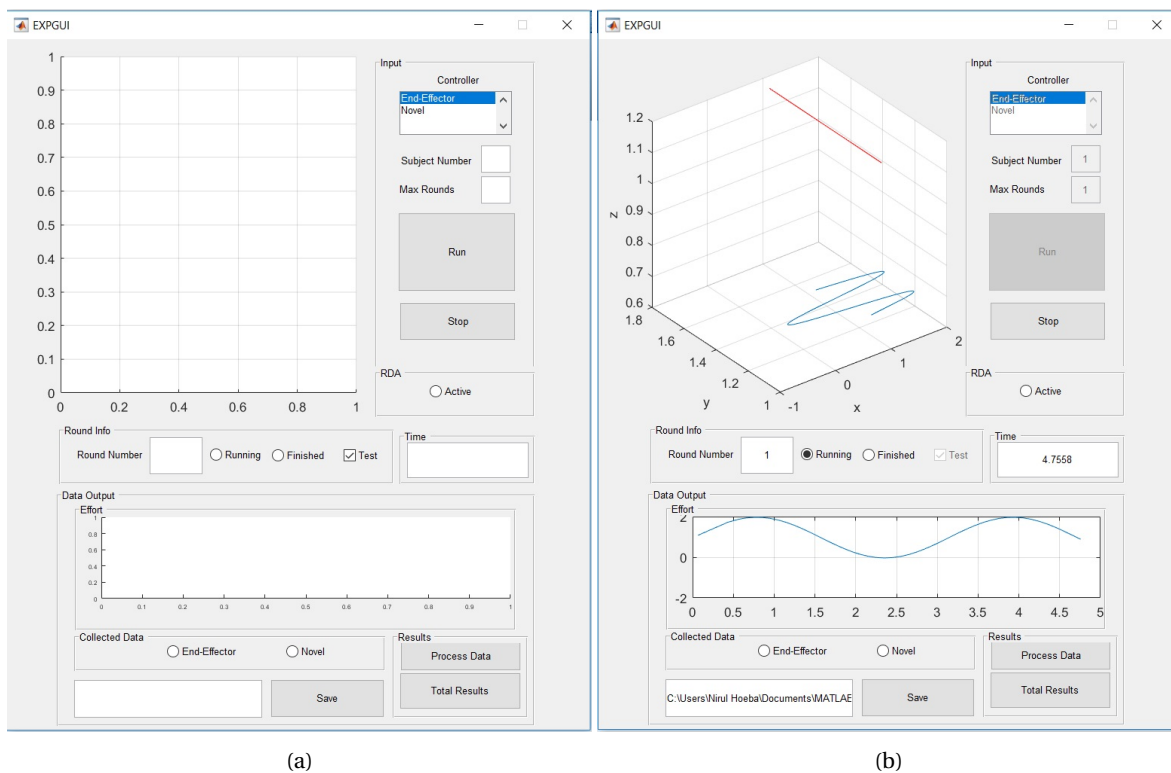
Figure C.1: (a) The interface capturing participant task performance data when deactivated and (b) activated

Appendix C.1 will give information about how participant experiment data was captured using an external computer as shown in Appendix B.1.

To capture participant experiment data, a laptop was used connected to the VR mediated framework using RDA. Task performance metric data sent from the VR environment to the external computer was captured using an interface created in MATLAB (Fig. C.1a and Fig. C.1b). This interface visualizes the captured data. After every experiment, raw data is processed using the interface and hereafter statistically analyzed and saved.

The interface requires information about:

- the participant number

- type of controller (condition)

- the number of trials (7 trials of which four are training trial and three experimental trials)

The interface automatically processes raw data of three experimental trials into one mean value per participants for:

- trajectory accuracy

- trajectory completion time

- the effort (work) on the control device

Subjective data was added to the raw data and processed data after the experiment using Fig.C.2a.

After every experiment, processed data used for the statistical analysis could be visualized in Fig. C.2b. Fig. C.2b shows the boxplots, user acceptance graph and a table with all the data from the statistically evaluated task performance and subjective data.

(a)

(b)

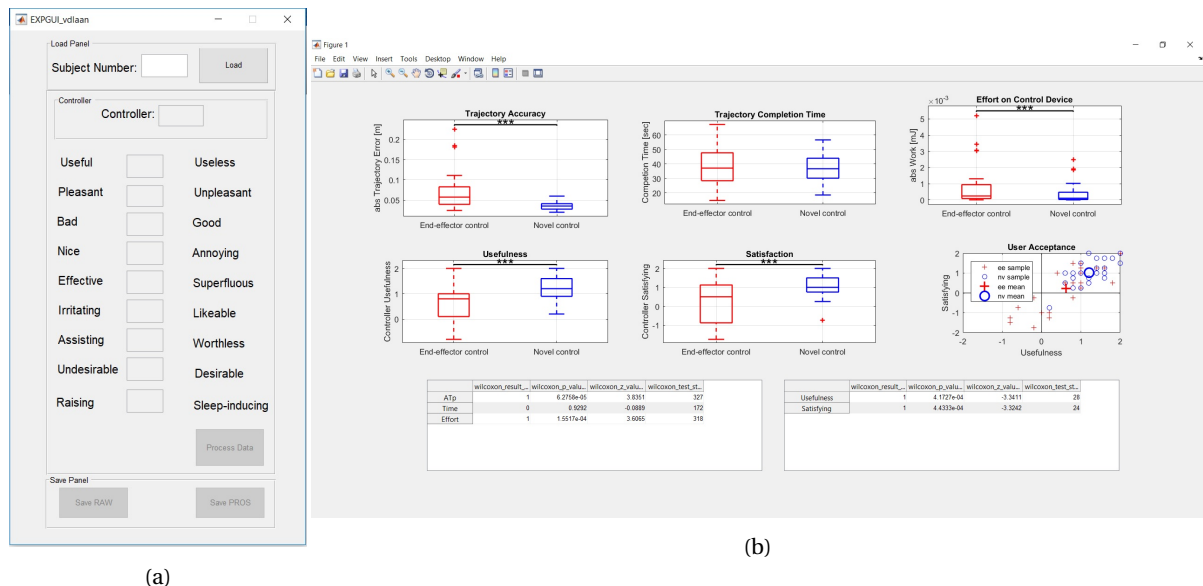Figure C.2: (a) The interface used to process and store subjective participant data. (b) Visualization of all statistically analyzed data in MATLAB.

D

ROS CONTROLLER SCHEME

Appendix D gives information about the control scheme used in the slave system as visualized in Fig. D.1. The scheme consists of nodes (ellipses) and topics (rectangles). Nodes represent processes that perform computations and communicate with each other using topics. The sections below will briefly describe the function of each node and the content of each topic.

D.1. NODES

GAZEBO
The node containing the end-effector and null-space controller. It uses these controllers to process input and compute output data. It communicates with the gazebo virtual environment reading poses, states, etc.

/RDA/ROS2RDA
The node that publishes topics to RDA.

/CONTROLLER2/VIVECONFIGCONTROLLER
The node that reads the pose information of the left control device from RDA.

/CONTROLLER1/VIVEEECONTROLLER
The node that reads the pose information of the right control device from RDA.

/CONTROLLER_SWITCHER
The node that switches the controller from novel to end-effector control or visa versa, dependent on the input of the dual-stage triggers of the right and left control devices.

/IIWA/IIWA_CART_CONVERTER
The node that calculates the error between the end-effector pose and the pose of the right control device.

/IIWA/IIWA_NULL_CONVERTER
The node that calculates the error between the end-effector pose and the end-effector target pose and converts the orientation of the left control device to a vector used to manipulate the four joint groups.

/IIWA/IIWA_STATE_MASTER
The node that registers all joint state and pose information of the iiwa 7 and register which invalid configurations occur.

/IIWA/CONTROLLER_SPAWNER
The node that spawns all controllers.

D.2. TOPICS

/IIWA/JOINT_STATES
Topic containing the joint states of all 7 iiwa joints.

/IIWA/IIWA_NULL_CONTROL/SINGULARVALUE
/IIWA/IIWA_CART_CONTROL/SINGULARVALUE
Topic containing a Boolean indicating if a singular joint configuration is attained.

/IIWA/IIWA_NULL_CONTROL/SMALLESTSINGULARVALUE_PRE
/IIWA/IIWA_CART_CONTROL/SMALLESTSINGULARVALUE_PRE
Topic containing the smallest singular value computed using the Singular Value Decomposition (SVD).

/IIWA/IIWA_NULL_CONTROL/ENDEFFECTORERROR
/IIWA/IIWA_CART_CONTROL/ENDEFFECTORERROR
Topic containing a Boolean indicating if the error between the commanded pose and the current end-effector pose is larger than zero.

/IIWA/IIWA_NULL_CONTROL/RESTART
/IIWA/IIWA_CART_CONTROL/RESTART
Topic containing a Boolean, which will become true when the control mode is switched. Temporary disabling the converter node of the deactivated controller.

/IIWA/IIWA_NULL_CONTROL/ENDEFFECTORTARGETPOSE
Topic containing the last detected/target pose of the end-effector before switching from end-effector control to novel control.

/IIWA/IIWA_NULL_CONTROL/ALPHACMD
Topic containing a vector (in the paper revered as, as ξ) containing information about which joint group should be rotated in which direction published by /iiwa/iiwa_null_converter.

/IIWA/IIWA_CART_CONTROL/ENDEFFECTORCMD
Topic containing the difference between the commanded pose (pose of the right controller) and the current end-effector position derived in the "/iiwa/iiwa_cart_converter" node.

/IIWA/IIWA_NULL_CONTROL/ENDEFFECTORCMD
Topic containing the difference between the last detected/target pose and the current end-effector position derived in the "/iiwa/iiwa_null_converter" node.

/CONTROLLER_CONFIG/USERTARGET/CLUTCH
Topic containing a Boolean indicating if the dual stag trigger of the left control device is pressed.

/CONTROLLER_EE/USERTARGET/CLUTCH
Topic containing a Boolean indicating if the dual-stage trigger of the right control device is pressed.

/CONTROLLER_CONFIG/USERTARGET/ALPHA
Topic containing a vector (in the paper revered as, as ξ) containing information about which joint group should be rotated in which direction. Published when null-space control is activated.

/CONTROLLER_CONFIG/USERTARGET/ALPHA_PRE
Topic containing a vector (in the paper revered as, as ξ) containing information about which joint group should be rotated in which direction which is always published to the control switcher node.

/CONTROLLER_EE/USERTARGET/POSE
Topic containing the pose of the right hand controller which is published when end-effector control is activated.

/CONTROLLER_EE/USERTARGET/POSE_PRE
Topic containing the pose of the right-hand controller which is always published

Figure D.1: ROS control scheme containing all nodes (processes) and topic (communication between processes) of the slave device system. Nodes that are faded, are nodes that are in the ROS control scheme but are not used for the experiment. The blue squares indicate the node where data enters the slave system. The green square indicates the node where the data leaves the slave system.

E

FORMS

E.1. EXPERIMENTAL INFORMATION

Experiment Information Form

PART 1: Thermology

Thank you for participating in this experiment. This section will introduce the robot arm and explain several terms used in this experiment.

The Robot Arm

The robot arm used in this experiment is the KUKA LBR iiwa 7 robot arm having 7 degrees of freedom (DOFs). In simple terms, 7 DOFs means that the robot has 7 rotating joints or small motors to adjust its posture. The position of all these joints is given in Fig. 1a. The tip or head of the robot is called its end-effector. The position of the end-effector is given in Fig. 1a and has coinciding centers with joint 7.

Workspace

The workspace of the robot is the nearby area surrounding the robot in which it can move and position its end-effector.

Joint Limit(s)

The seven joints of the robot arm rotate with respect to the base (i.e. the part standing on the ground). Because every part of the robot is connected to a joint, movement of a joint will result in the movement of all parts above these joints. The rotation of each joint is finite just like the rotation of our own joints is finite. A joint-limit is reached when a joint reaches its upper or lower joint limit and cannot move any further without breaking the robot. Reaching a joint limit will stop the movement of the robot. Movement is continued when the movement is in the opposite direction w.r.t. the joint limit.

Singularity

A singularity results in the reduction of DOFs when the robot is fully stretched or in a certain singular posture. In this experiment, singularities are of no importance but if they are attained the robot will stop moving.

Controllers

In this research, controllers are algorithms that are programmed to move the robot using the command given by you (i.e. the operator) using the control devices. This experiment will test two different controllers.

Control Device(s)

The control devices are the devices used to control the robot arm (Fig. 1b), which can be utilized with your hands. These control devices are a part of the HTC Vive virtual reality set.

(a)   (b)
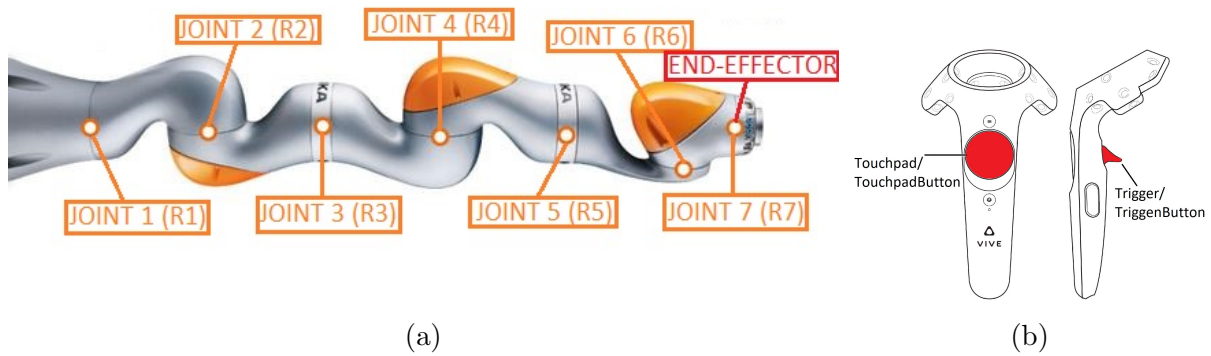
PART 2: Controlling the robot

In this part, we explain the control devices and how we can use these devices to control the robot arm.

Right-Hand Controller

The right-hand controller is responsible for the one-to-one mapping of controller motion to the end-effector. The end-effector is velocity controlled meaning that the motion executed by the end-effector is caused by the end-effector wanting to lower the error between previous and current position of the controller. Control of the end-effector is in global coordinates, meaning that for every configuration of the robot, the end-effector will move in the direction the controller moves. The controller has several buttons and triggers. Two of these buttons contain functions. These are the trigger and the touchpad button (Fig. 1b). Without pressing any trigger button, the end-effector of the robot will not move. Pressing the right-hand trigger will result in the translation and rotation of the end-effector equal to that of the controller. The touch-pad button is used in combination with the laser pointer emitted from this controller. When pressing the left-hand controller trigger a blue laser will emit from the right controller. This laser can be used as a pointer to press a button on the interface. When you are moving through the VR space without pressing the trigger, press the trigger twice to reset its position.

Interface

Hovering above the left controller is an interface (Fig. 2). This interface has seven (loading) bars and seven buttons. The bars and buttons both refer to the seven joints of the robot arm. The bars represent the amount of rotation (i.e. angle) of each respective joint between its upper limit (i.e. green plus sign) and its lower limit (i.e. red minus sign). The bars will change color to denote problems related to moving the robots. The bar will become **red** (Fig. 2) when the respective joint reaches its joint limit. The bar will become **magenta** when a singularity is reached. The interface will remain **green** (Fig. 2) if no problems are detected. This acts as visual feedback to see why the robot has stopped moving. Also, when a joint limit or singularity is attained, the left controlling device will lightly vibrate (tactile feedback). The buttons represent joint 1 (i.e. R1) until joint 7 (i.e. R7). Using the laser pointer a joint can be selected to change its configuration. In this experiment, only Button R1 will be activated.

Left-Hand Controller

The left-hand controller is responsible for the rotation of separate robotic joints. In this experiment you will only be able to rotate joint 1 (R1) for a fixed end-effector position. The controller has only one action button which is the trigger. When pressing the (left-)trigger the right-hand emits a blue laser beam with a pointer at the end (Fig. 2a). This pointer can be used to select a joint using the buttons on the interface (Fig. 2b). Pressing the left-hand trigger when a button is selected results in a curved red and green arrow surrounding the left controller and the respective joint on the robot arm (Fig. 2c). Rotating the left controller in the direction of the red or green arrow (like opening a door with a key) and keeping the left-trigger pressed will result in the rotation of the robot joint in the direction of the red or green arrow. A rotation in the direction of the red arrow will result in a rotation in the direction of the lower limit and a rotation in the direction of the green arrow in the direction of the upper limit.

(a)　　　　　　　　　　(b)　　　　　　　　　　(c)
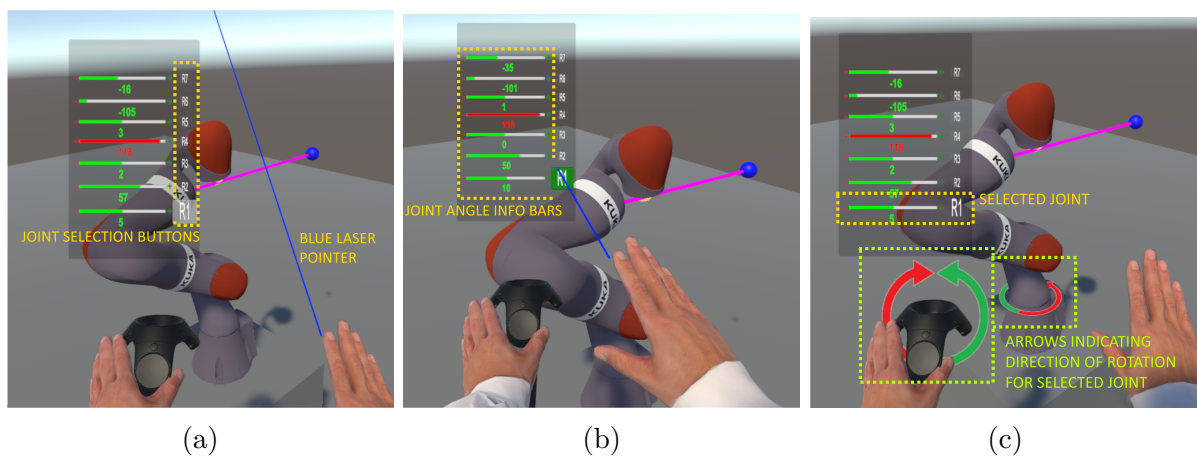
Figure 2

PART 3: The Task

Operation of a robot arm consists mainly of translating the end-effector from one location to another in the workspace, preferably using the shortest path. Your task will operate the end-effector of the robot from one position to another by following a predefined trajectory as accurate as possible within a time frame of two minutes. High accuracy is defined as low error between the end-effector path and the predefined trajectory. Fig. 3 and Fig. 4 visualizes the trajectory where the green sphere denotes the begin position, the magenta colored line is the defined trajectory and the red sphere is the final position.

When operating the end-effector from the start to the finish, at 3/4 of the path the robot stops moving due to joint 4 (i.e. R4) which has reached its lower joint limit. The experiment will measure how you solve this problem by using two controllers. There is a lag between the your input and the output of the robot. Please keep this in mind.

PART 4: The Experiment

Training session 1

Training session 1 will be used to train you using the first controller. In this training session, you will follow the trajectory until you will reach a joint limit, after which moving in the direction of the red (finish) sphere is not possible using the same posture. After reaching this limit you have to find a solution to translate the end-effector so that it can reach the red sphere. After successful training, you will do the experiment.

Experiment 1

Experiment 1 will evaluate your ability in following the trajectory as accurate as possible using controller 1 which has the ability to translate and rotate the end-effector using **ONLY** the right-hand controller. In this experiment, the interface is enabled, enabling visual and tactile feedback when a joint limit is attained. Figure 3 shows an example of the several steps of the experiment. From the start position (Fig. 3 .START), you move downwards as accurate as possible. After reaching the joint limit configuration try to find a solution or alternative path to reach the red finish (sphere) by translating and rotating the end-effector. If you think that movement to the red (finish) sphere is not possible due to the joint-limit you **MAY** deviate form the magenta colored path.
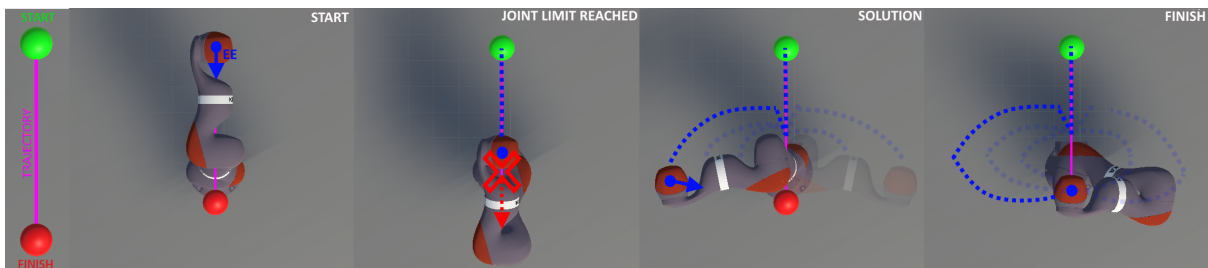
Figure 3

Training session 2

This session is equal to the first training session, only in this training session you will train you using the second controller. Using this controller you should adjust the robotic posture in such a way that you can reach the red sphere after a joint limit.

Experiment 2

Experiment 2 will evaluate your ability in following the trajectory as accurate as possible. In this experiment you will use **BOTH** control devices. Where the right-hand control device has to ability to translate the end-effector. The left-hand control device has the ability to and adjust the robotic joint posture by using the interface and left-hand controller to rotate around the first joint (R1) (Fig. 4.SOLUTION). In this experiment the interface is enabled, enabling visual and tactile feedback. From the start position (Fig. 4.START), you move downwards as accurate as possible. After reaching the joint limit configuration, try to find a solution to reach the red sphere (finish) by changing the joint posture using the interface.

Figure 4

Questionnaire

After every experiment, you will be asked to fill in a questionnaire assessing your opinion about the controller used for the task. After the experiments, I will ask you which controller you preferred.

PART 5: The Summary

- The robot arm is a linkage of multiple segments with rotating joints between the segments. When rotating one segment, all segments above this segment will also move.

- Each joint can rotate for a finite amount between its upper and lower limit. When a limit is reached, the controller stops the motion.
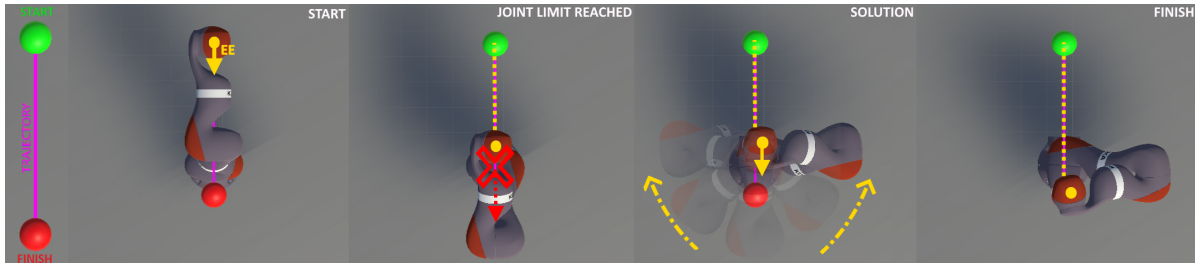
- To control the robot, two HTC Vive controllers are used. The right controller is used to move the head or end-effector of the robot. When moving the end-effector all segments below the end-effector will also move (because these position the end-effector in 3D-space). The left controller will, after you select joint 1 (R1) on the interface, enable you to rotate the whole arm with respect to its base.

- Your task is to move the end-effector of the robot from the green (begin) sphere to the red (finish) sphere remaining as close as possible to the magenta colored trajectory. If you think that moving to finish sphere is not possible anymore when following the magenta trajectory due to a joint-limit, you **should** and **may** deviate from the magenta colored trajectory to eventually reach the red (finish) sphere.

- For both experiments the task will remain the same, but for both experiments, you will use a different controller. After every experiment, you will be asked to fill in a questionnaire and after both experiments, you will be asked which controller you preferred more.

- Control of the end-effector is in global coordinates, meaning that no matter the posture or configuration of the robot, movement of your control device in for example south direction will always result in the robot end-effector/head moving in south direction.

- The experiment will take ± 30 minutes.

E.2. INFORMED CONSENT FORM

Informed Consent Form for the Human Subjects Experiment

This Informed Consent Form is written for men and women who attend the human subject's experiment. The title of our research project is "Development and validation of a controlling algorithm suitable for the VR mediated teleoperation of a redundant KUKA LBR iiwa 7 used in free-air movement applications by exploring the robot arm null-space."

Principal Investigator:	Hoeba, N.S. (Nirul)
Organization:	TNO and TU Delft
Sponsor:	TNO
Version:	V1

This Informed Consent Form has two parts:
- **Information Sheet (to share information about the research with you**
- **Certificate of Consent (for signatures if you agree to take part)**

You will be given a copy of the full Informed Consent Form

PART 1: Information Sheet

Introduction
My name is Nirul Hoeba and I am doing my graduation project at TNO and the TU Delft to obtain my Master of Science (MSc.) for the study Mechanical Engineering at the Technical University of Delft (TU Delft). We are researching on controlling capabilities of a human operator of a robotic arm in trajectory tracking tasks using the KUKA LBR iiwa 7 robotic arm. This form will inform you about the research and will invite you to be a part of this research. Before you decide, you can talk to anyone you feel comfortable with about the research. If there are words or parts of this inform consent form that you do not understand. Please ask me to stop as we go through the information and I will take the time to explain. If you have questions later, you can always ask them to me using my contact information mentioned at the section "Contact Information".

Purpose of the research
The purpose of the research is to validate a newly developed algorithm for the teleoperation of the KUKA LBR iiwa 7 robot arm in a virtual reality (VR) environment operated by a human operator.

Benefits and risks of participating
There are no known direct risks for this experiment. Participants might feel mild nauseating sensations during the experiments due to "motion sickness". Motion sickness can be caused by the virtual reality environment, but because the experiments are short with a break between the sessions and accurate calibration was done between the human motion and avatar motions the probability of these effects to happen are very low.

If you participate in this research, you will have the following benefits: hands-on experience in teleoperating a robot arm, experience in human-robot interaction experiments and the possibility to help future robots systems develop better interfaces due to your participation.

Confidentiality

The information that we collect from this research project will be kept confidential. Information about you that will be collected during the research will be put away and no-one but the researchers will be able to access it. Any information about you will be anonymized and will have a number instead of your name and no personal data will be recorded. Only information related and obtained via this experiment will be used. The obtained data will be processed by the researchers only. At the end of the research, a copy of all data will be provided to the TU Delft. There is a possibility for the collected data to be published in a paper or/and thesis. This will be done respecting your anonymity.

Right to Refuse or Withdrawal

You do not have to take part in this research if you do not wish to do so. You may stop participating in the research at any time that you wish without any consequences. It is your choice and that choice will be respected.

Contact Information

As mentioned in the introduction, if you have questions you may ask them now, later or after the study has started. If you wish to ask questions later you can contact Nirul Hoeba using the information given below. For any other question related to TNO or TU Delft or to file a complaint against the experimenter, you can contact respectively dr. Nanda van der Stap (TNO) and prof. dr. ir. David Abbink (TU Delft).

Name:	Nirul Hoeba	dr. Nanda van der Stap	prof. dr. ir. David Abbink
Address:	Oude Waalsdorperweg 63	Oude Waalsdorperweg 63	Mekelweg 2
Postcode:	2597 AK Den Haag	2597 AK Den Haag	2628 CD Delft
Tel:	0646471565	-	-
Email:	nirul.hoeba@tno.nl	nanda.vanderstap@tno.nl	d.a.abbink@tudelft.nl

PART 2: Certificate of Consent

Please mark the appropriate boxes	Yes	No
Taking part in the study		

Taking part in the study

I have read and understood the study information dated [/   /   ], or it has been read to me. I have been able to ask questions about the study and my questions have been answered to my satisfaction. ○ ○

I consent voluntarily to be a participant in this study and understand that I can refuse to answer questions and I can withdraw from the study at any time, without having to give a reason. ○ ○

I understand that taking part in the study involves the operation of a robot arm in a VR environment using the HTC Vive virtual reality system. ○ ○

Risks associated with participating in the study

I understand that taking part in the study can possibly involve the following risks: *Motion Sickness causing mild nauseating feelings.* ○ ○

Use of the information in the study

I understand that the information I provide will be used for: *reports, publications, and data processing.* ○ ○

I understand that personal information collected about me that can possibly identify me, such as, performance and effort parameters will be anonymized and will not be shared beyond the study team and the TU Delft. ○ ○

Signatures

_____   _____   _____

Name of participant [printed]   Signature   Date

For participants unable to sign their name, mark the box instead of sign

I have witnessed the accurate reading of the consent form with the potential participant and the individual has had the opportunity to ask questions. I confirm that the individual has given consent freely.

_____   _____ _____

Name of witness   [printed]   Signature   Date

I have accurately read out the information sheet to the potential participant and, to the best of my ability, ensured that the participant understands to what they are freely consenting.

_____   _____   _____

Name of participant [printed]   Signature   Date

E.3. Van der Laan (Acceptance) Questionnaire

Van der Laan Questionnaire

This questionnaire assesses the acceptance of the system that you have used during the experiment.

Participant nr:	Date:	Controller:

I find controlling the robot arm using this controller (please tick a box on every line)

1.	Useful		Useless
2.	Pleasant		Unpleasant
3.	Bad		Good
4.	Nice		Annoying
5.	Effective		Superfluous
6.	Irritating		Likeable
7.	Assisting		Worthless
8.	Undesirable		Desirable
9.	Raising Alertness		Sleep-inducing

Please enter further comments on the controller below:

E.4. PARTICIPANT CONDITION ORDER AND USER CONTROLLER PREFERENCE TABLE

Subject Nr.		Experiment 1	Questionnaire 1		Experiment 2	Questionnaire 2		Preferred Controlleer
1		1	1		2	2		2
2		2	2		1	1		2
3		1	1		2	2		2
4		2	2		1	1		2
5		1	1		2	2		2
6		2	2		1	1		2
7		1	1		2	2		2
8		2	2		1	1		2
9		1	1		2	2		2
10		2	2		1	1		2
11		1	1		2	2		2
12		2	2		1	1		2
13		1	1		2	2		1
14		2	2		1	1		1
15		1	1		2	2		2

16		2	2		1	1		2
17		1	1		2	2		2
18		2	2		1	1		1
19		1	1		2	2		2
20		2	2		1	1		1
21		1	1		2	2		2
22		2	2		1	1		1
23		1	1		2	2		2
24		2	2		1	1		2
25		1	1		2	2		2
26		2	2		1	1		2